EUROPEAN JOURNAL OF PURE AND APPLIED MATHEMATICS
2025, Vol. 18, Issue 4, Article Number 6042
ISSN 1307-5543 – ejpam.com
Published by New York Business Global

A Novel Explicit Two-Derivative Runge-Kutta-Nyström Method with Energy Conservation for the Integration of Second-Order Periodic ODEs

Zhuoyu Sun[1,*], K.C. Lee[1,*], N.H.A. Aziz[3], I. Hashim[1], M.A Alias[1], N. Senu[2,4]

[1] *Department of Mathematical Sciences, Universiti Kebangsaan Malaysia, 43600 UKM Bangi, Selangor, Malaysia*
[2] *Institute for Mathematical Research, Universiti Putra Malaysia, 43400 UPM, Serdang, Malaysia*
[3] *Department of Mathematical Sciences, Faculty of Intelligent Computing, Universiti Malaysia Perlis (UniMAP), Kampus Alam UniMAP Pauh Putra, 02600 Arau, Perlis, Malaysia*
[4] *Department of Mathematics and Statistics, Universiti Putra Malaysia, 43400 UPM, Serdang, Malaysia*

Abstract. A novel trigonometrically-fitted explicit two-derivative Runge-Kutta-Nyström (TFETDRKN(5)) method with three-stage and fifth-order for solving a class of special second-order (system) ODEs in the form of $u'' = f(t, u)$ with periodic solutions is proposed. Order conditions of the new explicit two-derivative Runge-Kutta-Nyström (ETDRKN(5)) method are derived using Taylor expansion and comparison of step size, h over Taylor method and general formula of the ETDRKN(5) method. Trigonometrically-fitting technique is implemented into the ETDRKN(5) method to form the TFETDRKN(5) method. Stability analysis of the new proposed method is thoroughly investigated and discussed. Algebraic order of the ETDRKN(5) method is investigated. Numerical experiments for the TFETDRKN(5) method are conducted versus error accuracy, number of function evaluations and computational time. Numerical tables and graphs demonstrate that the TFETDRKN(5) method has higher effectiveness and accuracy compared to selected existing methods. Further study for one typical real-word experiment is conducted. Besides, Hamiltonian energy, Lagrangian energy and momentum conservation of proposed method are investigated to outlook the energy conservation property. The related energy exchange of the above three energies during the tested real-world experiment is illustrated.

2020 Mathematics Subject Classifications: 65L05, 65L06, 65L20, 70H12
Key Words and Phrases: Second-order ordinary differential equations, trigonometrical integration, explicit two-derivative Runge-Kutta-Nyström method, stability analysis, algebraic order analysis, energy conservation

*Corresponding author.
*Corresponding author.
DOI: https://doi.org/10.29020/nybg.ejpam.v18i4.6042

Email addresses: a2408527882@163.com (Z. Sun),
kclee_1017@ukm.edu.my (K. C. Lee)

1. Introduction

In this study, We consider the special second-order ordinary differential equations (ODEs)

$$\begin{aligned}&u''(t) = f(t, u(t)),\ u(t_0) = u_0,\ u'(t_0) = u'_0,\\&u : \mathbb{R} \to\ \mathbb{R}^k,\ \ f : \mathbb{R} \times\ \mathbb{R}^k \to\ \mathbb{R}^k,\ \ t \in [t_0, t_{end}].\end{aligned} \tag{1}$$

Second-order ODEs with periodic solutions are common in many scientific and engineering fields, modeling systems with inherent periodic behavior. These equations are used in applications such as mechanical oscillators, electrical circuits with inductors and capacitors, and molecular vibrations, capturing the essential dynamics of systems that exhibit regular oscillations (see [1],[2] and so on).

In the beginning, Runge-Kutta (RK) methods were designed to solve the first-order ODEs [3, 4]. With the development, Nyström [5] extended RK methods to second-order ODEs, now known as Runge-Kutta-Nyström (RKN) methods, building upon the original ideas of his predecessors. Compared with the general RK methods solving first order ODEs, RKN methods are designed specifically for second-order ODEs, which makes them more efficient and accurate for such types of problems. They use both the first and second derivatives of the solution, which helps to achieve higher accuracy. However, many standard RKN methods do not account for the property of periodic solutions, often leading to unsatisfactory numerical results. To address this, many researchers have attempted to modify RKN methods by incorporating trigonometrically fitting techniques. Among these efforts, some have proven highly successful. The main idea behind trigonometrically fitted methods is to seek an exact integration for differential equations whose solutions can be expressed as linear combinations of certain functions $\{\cos(\lambda t),\ \sin(\lambda t),\ \lambda > 0\}$. Paternoster [6] considered the construction of RKN methods for ODEs with oscillatory solutions and derived RK and RKN methods which integrate trigonometric polynomials exactly by using the linear stage representation of a RK method given in Albrecht's approach [7]. Franco [8] constructed new explicit RKN methods up to order 5, specially adapted to the numerical integration of perturbed oscillators. Li [9] developed fifth and sixth-order trigonometrically fitted three-derivative Runge-Kutta (TFTHDRK) by using rooted trees theory and B-series. At the same year, Li et al. [10] Extended explicit pseudo two-step Runge–Kutta–Nyström (EEPTSRKN) methods have been proposed for the numerical integration of oscillatory systems, inheriting the framework of the explicit pseudo two-step Runge-Kutta-Nyström methods. These methods are designed to integrate exactly the unperturbed problem $y'' + My = 0$, achieve a maximum step order of $s + 2$ and stage order of $s + 1$.

And very recently, Demba et al. successively developed explicit, embedded explicit, phase- and amplification-fitted 5(4) diagonally explicit, phase- and amplification-fitted 5(4) diagonally implicit Runge-Kutta-Nyström methods, making a significant contribution to the progress of trigonometrical integration research (see[11–14] for further details). These advancements in RKN methods hava significantly improved the efficiency and accuracy of solving oscillatory and periodic initial value problems. Several developing methods, including the fourth-order four-stage explicit trigonometrically-fitted RKN methods, demonstrate smaller global errors compared to existing methods [11]. Embedded pairs, such as the 4(3) explicit trigonometrically-fitted RKN methods, offer reduced computational costs with fewer function evaluations per step [12]. Additionally, phase- and amplification-fitted methods have been developed, maintaining high-order convergence and providing improved stability intervals [13]. Notably, the PFAFRKN5(3) and PFAF-DIRKN5(4)4 pairs show enhanced accuracy and efficiency over their counterparts, offering promising results for solving complex oscillatory problems [14].

Motivated by the goal of enhancing the order and numerical accuracy of RKN methods, many researchers have modified the classical RKN methods into two-derivative Runge-Kutta-Nyström (TDRKN) methods by incorporating the second derivatives of f-evaluation into the formulation. Chen et al. [15] extended the traditional RKN methods for general second-order ODEs to TDRKN methods involving the third derivative. The order criteria for TDRKN methods were derived using a novel version of Nyström tree theory and the associated B-series theory. They developed a two-stage explicit TDRKN method of fourth-order and a three-stage explicit TDRKN method of fifth-order. Jator [16] introduced a trigonometrically-fitted implicit third derivative Runge-Kutta-Nyström method (TTRKNM), with coefficients dependent on the frequency and step size, for periodic initial value problems (IVPs). The TTRKNM consists of a pair of methods derived from its continuous version, which are used to produce simultaneous approximations of the solution and its first derivative at each point in the interval of interest. The stability properties of the method were discussed, and numerical experiments were conducted to demonstrate its accuracy and efficiency. Chen et al. [17] proposed a new family of modified TDRKN methods for solving second-order oscillatory ODEs. Order conditions were derived using Nyström tree theory and B-series theory. They established trigonometrically-fitted conditions and constructed two practical explicit trigonometrically-fitted TDRKN (TFTDRKN) methods. The phase properties of the new integrator were examined, and their periodicity regions were determined. Numerical experiments demonstrated the efficiency and competence of the new methods. For a comprehensive discussion on the construction and analysis of trigonometrically-fitted or exponentially-fitted TDRKN methods, readers are directed to the works in [18–20] and so on.

Among articles about solving second-order ODEs using TDRKN methods, those addressing general second-order ODEs account for the vast majority. There are numerous RKN methods for integrating a general class of second-order IVPs. However, there is a lack of research applying TDRKN methods to solving special classes of second-order ODEs in the form of $u'' = f(t, u)$. Additionally, there is a shortage of studies on constructing trigonometrically-fitted TDRKN methods for directly solving special classes of second-order ODEs with periodic solutions. Hence, we focus on developing a new efficient trigonometrically-fitted TDRKN (TFETDRKN(5)) method with high effectiveness and accuracy and energy conservation for solving special classes of second-order periodic ODEs like (1).

In sections 2 and 3 we construct a new ETDRKN(5) method with three-stage and fifth-order. In section 4 we apply the trigonometrically-fitting technique to the ETDRKN(5) method to derive the TFETDRKN(5) method, which constitutes the primary focus of this study. In section 5 we conduct a thorough stability analysis of the TFETDRKN(5) method involving stability matrix, dispersion and dissipation error analysis, and stability properties and regions. In section 6 we prove the algebraic order of the ETDRKN(5) method is 5. In sections 7 and 8 we conduct numerical experiments for the TFETDRKN(5) method against error accuracy, number of function evaluations and computational time compared with some existing similar methods to demonstrate that the TFETDRKN(5) method has higher accuracy and effectiveness. In section 9 we demonstrate the enhanced accuracy and energy conservation of the ETDRKN(5) method, which is achieved by employing the trigonometrical integration technique. Section 10 is dedicated to the concluding remarks.

2. The Formulation of the Two-Derivative Runge-Kutta-Nyström Method

The TDRKN method is a numerical technique designed to solve second-order ODEs. These methods are extensions of standard Runge-Kutta (Runge-Kutta-Nyström) methods tailored for second-order ODEs (system), making them highly effective for problems involving dynamics like mechanical systems, wave motion, or electrical circuits. The key advantage of TDRKN methods lies in their ability to directly handle second-order ODEs by using both position and velocity (or their equivalents) in the system and incorporate higher-order accuracy while maintaining computational efficiency, leading to greater efficiency and accuracy compared to traditional methods that require transforming the system into a set of first-order equations.

Letting $u'''(t) = g(t, u(t), u'(t))$ and combining $u''(t) = f(t, u(t))$ in the problem (1), we can convert this problem to the following form

$$\begin{pmatrix} u''(t) \\ f'(t, u(t)) \end{pmatrix} = \begin{pmatrix} f(t, u(t)) \\ g\left(t, u(t), u'(t)\right) \end{pmatrix}, \quad \begin{pmatrix} u(t_0) \\ f(t_0, u(t_0)) \end{pmatrix} = \begin{pmatrix} u_0 \\ u''_0 \end{pmatrix}. \tag{2}$$

The two-derivative Runge-Kutta-Nyström (TDRKN(5)) method with s-stage, which is developed by incorporating the third derivative, $u'''(t)$ into the formulation, is illustrated as

$$\begin{aligned}
u_{n+1} &= u_n + hu'_n + \frac{h^2}{2} f(t_n, u_n) + h^3 \sum_{i=1}^{s} \bar{d}_i g\left(t_n + c_i h, U_i, U'_i\right), \\
u'_{n+1} &= u'_n + hf(t_n, u_n) + h^2 \sum_{i=1}^{s} \tilde{d}_i g\left(t_n + c_i h, U_i, U'_i\right), \\
U_i &= u_n + c_i h u'_n + \frac{1}{2}(c_i h)^2 f(t_n, u_n) + h^3 \sum_{i=1}^{s} \bar{A}_{ij} g\left(t_n + c_i h, U_j, U'_j\right), \\
U'_i &= u'_n + c_i h f(t_n, u_n) + h^2 \sum_{i=1}^{s} \tilde{A}_{ij} g\left(t_n + c_i h, U_j, U'_j\right),
\end{aligned} \tag{3}$$

where $c_i, \bar{d}_i, \tilde{d}_i, \bar{A}_{ij}, \tilde{A}_{ij}, i = 1, \cdots, s$ are real numbers. The scheme (3) can be expressed as in Kronecker's block product notation:

$$\begin{aligned}
&u_{n+1} = u_n + hu'_n + \frac{h^2}{2} f(t_n, u_n) + h^3 \left(\bar{d} \otimes I_{k\times k}\right) G\left(U, U'\right), \\
&u'_{n+1} = u'_n + hf(t_n, u_n) + h^2 \left(\tilde{d} \otimes I_{k\times k}\right) G\left(U, U'\right), \\
&U = u_n + h\left(c \otimes u'_n\right) + \frac{1}{2} h^2 \left(cc^T \otimes f(t_n, u_n)\right) + h^3 \left(\bar{A} \otimes I_{k\times k}\right) G\left(U, U'\right), \\
&U' = e \otimes u'_n + h\left(c^T \otimes f(t_n, u_n)\right) + h^2 \left(\tilde{A} \otimes I_{k\times k}\right) G\left(U, U'\right),
\end{aligned} \tag{4}$$

where $e = (1, \cdots, 1)^T$, $c = (c_1, \cdots, c_s)^T$, $\bar{d} = \left(\bar{d}_1, \cdots, \bar{d}_s\right)$, $\tilde{d} = \left(\tilde{d}_1, \cdots, \tilde{d}_s\right)$ are s-dimensional vectors, $\bar{A} = \left(\bar{A}_{ij}\right)_{s\times s}$, $\tilde{A} = \left(\tilde{A}_{ij}\right)_{s\times s}$ are $s \times s$ matrices and $I_{k\times k}$ is $k \times k$ identity matrix. The block vectors in $\mathbb{R}^{s\times k}$ are

$$U = (U_1, \cdots, U_s), \; U' = (U'_1, \cdots, U'_s), \; G(U, U') = (g(t_0 + c_1 h, U_1, U'_1), \; \cdots, g(t_0 + c_s h, U_s, U'_s)). \tag{5}$$

An alternative expression of the scheme (3) is given as follows:

$$\begin{aligned}
&u_{n+1} = u_n + hu'_n + \frac{h^2}{2} f(t_n, u_n) + h^3 \sum_{i=1}^{s} \bar{d}_i l_i, \\
&u'_{n+1} = u'_n + hf(t_n, u_n) + h^2 \sum_{i=1}^{s} \tilde{d}_i l_i,
\end{aligned} \tag{6}$$

where

$$l_i = g\left(t_n + c_i h, \; u_n + c_i h u'_n + \frac{1}{2}(c_i h)^2 f(t_n, u_n) + h^3 \sum_{i=1}^{s} \bar{A}_{ij} l_j, \; u'_n + c_i h f(t_n, u_n) + h^2 \sum_{i=1}^{s} \tilde{A}_{ij} l_j\right). \tag{7}$$

It is convenient to represent the scheme (3) using the following Butcher tableau:

Table 1: Butcher Tableau for the TDRKN(5) method.

$$\begin{array}{c|c|c}
c & \bar{A} & \tilde{A} \\
\hline
 & \bar{d} & \tilde{d}_i
\end{array}$$

The TDRKN(5) method is explicit if $\bar{A}_{ij} = 0$, $\tilde{A}_{ij} = 0$ for $i \leqslant j$ and implicit if $\bar{A}_{ij} \neq 0$, $\tilde{A}_{ij} \neq 0$ for $i \leqslant j$ and involves only one evaluation of f and many g evaluations of per step. We select to construct a new explicit method, named as the ETDRKN(5) method.

3. Construction of the Fifth-Order Efficient Two-Derivative Runge-Kutta-Nyström Method

First, we utilize the Taylor series expansion to determine the coefficients of the ETDRKN(5) method of three-stage and fifth-order. By equating this expansion to the theoretical solution, which is also represented by a Taylor series, and performing some simplifying assumptions, we derive a system of non-linear equations via Maple. These equations are known as the order conditions of the ETDRKN(5) method.

The order conditions for u:
Third-order:

$$\sum_{i=1}^{3} \bar{d}_i = \frac{1}{6}. \tag{8}$$

Fourth-order:

$$\sum_{i=1}^{3} \bar{d}_i c_i = \frac{1}{24}. \tag{9}$$

Fifth-order:

$$\sum_{i=1}^{3} \bar{d}_i {c_i}^2 = \frac{1}{60}. \tag{10}$$

Sixth-order:

$$\sum_{i=1}^{3} \bar{d}_i {c_i}^3 = \frac{1}{120}, \tag{11a}$$

$$\sum_{i=1}^{3} \left(\sum_{j=1}^{i-1} \bar{d}_i \bar{A}_{ij} \right) = \frac{1}{720}, \tag{11b}$$

$$\sum_{i=1}^{3} \left(\sum_{j=2}^{i-1} \bar{d}_i \bar{A}_{ij} c_j \right) = \frac{1}{720}. \tag{11c}$$

The order conditions for u':
Second-order:

$$\sum_{i=1}^{3} \tilde{d}_i = \frac{1}{2}. \tag{12}$$

Third-order:

$$\sum_{i=1}^{3} \tilde{d}_i c_i = \frac{1}{6}. \tag{13}$$

Fourth-order:

$$\sum_{i=1}^{3} \tilde{d}_i {c_i}^2 = \frac{1}{12}. \tag{14}$$

Firth-order:

$$\sum_{i=1}^{3} \tilde{d}_i {c_i}^3 = \frac{1}{20}, \tag{15a}$$

$$\sum_{i=1}^{3} \left(\sum_{j=2}^{i-1} \tilde{d}_i \tilde{A}_{ij} c_j \right) = \frac{1}{120}, \tag{15b}$$

$$\sum_{i=1}^{3} \left(\sum_{j=1}^{i-1} \tilde{d}_i \bar{A}_{ij} \right) = \frac{1}{120}. \tag{15c}$$

Sixth-order:

$$\sum_{i=1}^{3} \tilde{d}_i {c_i}^4 = \frac{1}{30}, \tag{16a}$$

$$\sum_{i=1}^{3} \left(\sum_{j=1}^{i-1} \tilde{d}_i c_i \bar{A}_{ij} \right) = \frac{1}{180}, \tag{16b}$$

$$\sum_{i=1}^{3} \left(\sum_{j=2}^{i-1} \tilde{d}_i \bar{A}_{ij} c_j \right) = \frac{1}{720}, \tag{16c}$$

$$\sum_{i=1}^{3} \left(\sum_{j=2}^{i-1} \tilde{d}_i \tilde{A}_{ij} {c_j}^2 \right) = \frac{1}{360}, \tag{16d}$$

$$\sum_{i=1}^{3} \left(\sum_{j=2}^{i-1} \tilde{d}_i c_i \tilde{A}_{ij} c_j \right) = \frac{1}{180}. \tag{16e}$$

Referring to idea of reducing the number of N-trees required for order conditions obtained in [15], we propose the following relations

$$\begin{aligned} (t_0 + c_i h)^2 &= {t_0}^2 + 2t_0 \cdot (c_i h) + (c_i h)^2 = {t_0}^2 + \int_{t_0}^{t_0+c_i h} 2t_0 d\tau + \int_{t_0}^{t_0+c_i h} \int_{t_0}^{\tau} 2 d\sigma d\tau, \\ (t_0 + c_i h)^3 &= {t_0}^3 + 3{t_0}^2 \cdot (c_i h) + 3t_0 \cdot (c_i h)^2 + (c_i h)^3 \\ &= {t_0}^3 + \int_{t_0}^{t_0+c_i h} 3{t_0}^2 d\tau + \int_{t_0}^{t_0+c_i h} \int_{t_0}^{\tau} 6t_0 d\sigma d\tau + \int_{t_0}^{t_0+c_i h} \int_{t_0}^{\tau} \int_{t_0}^{\sigma} 6 d\varsigma d\sigma d\tau, \end{aligned} \tag{17}$$

which yield the simplifying assumptions

$$\tilde{A}e = \frac{1}{2}c^2,\ \bar{A}e = \frac{1}{6}c^3,\ \text{i.e.,}\ \sum_{j=1}^{s} \tilde{A}_{ij} = \frac{1}{2}{c_i}^2,\ \sum_{j=1}^{s} \bar{A}_{ij} = \frac{1}{6}{c_i}^3. \tag{18}$$

We utilize the order conditions (8-15c,12-15c,11a) and simplifying assumptions (18) ($i = 2, j = 1$) to generate the coefficients of the ETDRKN(5) method which are presented in the following Butcher tableau:

Table 2: Butcher Tableau for the ETDRKN(5) method with three-stage and fifth-order.

$$\begin{array}{c|ccc|ccc} 0 & 0 & 0 & 0 & 0 & 0 & 0 \\ c_2 & \bar{A}_{21} & 0 & 0 & \tilde{A}_{21} & 0 & 0 \\ c_3 & \bar{A}_{31} & \bar{A}_{32} & 0 & \tilde{A}_{31} & \tilde{A}_{32} & 0 \\ \hline & \bar{d}_1 & \bar{d}_2 & \bar{d}_3 & \tilde{d}_1 & \tilde{d}_2 & \tilde{d}_3 \end{array}$$

After solving the order conditions mentioned above, we obtains the solution with one free coefficient $\bar{A}_{31}$ as follow:

$$\bar{A}_{32} = -\bar{A}_{31} + \frac{1}{30} - \frac{\sqrt{5}}{75}. \tag{19}$$

Then, we generate all coefficients of the ETDRKN(5) method:

$$\begin{aligned} & c_1 = 0,\ c_2 = \frac{1}{2} + \frac{\sqrt{5}}{10},\ c_3 = \frac{1}{2} - \frac{\sqrt{5}}{10}, \\ & \bar{A}_{21} = \frac{1}{30} + \frac{\sqrt{5}}{75},\ \bar{A}_{32} = \bar{A}_{31} + \frac{1}{30} - \frac{\sqrt{5}}{75},\ \tilde{A}_{21} = \frac{3}{20} + \frac{\sqrt{5}}{20},\ \tilde{A}_{31} = 0,\ \tilde{A}_{32} = \frac{3}{20} - \frac{\sqrt{5}}{20}, \\ & \bar{d}_1 = \frac{1}{24},\ \bar{d}_2 = \frac{1}{16} - \frac{\sqrt{5}}{48},\ \bar{d}_3 = \frac{1}{16} + \frac{\sqrt{5}}{48},\ \tilde{d}_1 = \frac{1}{12},\ \tilde{d}_2 = \frac{5}{24} - \frac{\sqrt{5}}{24},\ \tilde{d}_3 = \frac{5}{24} + \frac{\sqrt{5}}{24}. \end{aligned} \tag{20}$$

Euclidean norms (2-norms) [21] of the error terms for the sixth-order approximations of u and u' of the ETDRKN(5) method are defined as

$$\left\|\tau^{(6)}\right\|_2 = \sqrt{\sum_{i=1}^{K}\left(\tau_i^{(6)}\right)^2},\ \left\|\tau'^{(6)}\right\|_2 = \sqrt{\sum_{i=1}^{L}\left(\tau_i'^{(6)}\right)^2},\ \left\|\tau_g^{(6)}\right\|_2 = \sqrt{\sum_{i=1}^{K+L}\left[(\tau_i^{(6)})^2 + (\tau_i'^{(6)})^2\right]}, \tag{21}$$

where K and L are the total number of local truncation errors for u and u', $\tau^{(6)}$ and $\tau'^{(6)}$ are the sixth-order local truncation error norms for u and u' respectively, and $\left\|\tau_g^{(6)}\right\|_2$ is sixth-order global truncation error norm used to decide the values of $\bar{A}_{31}$ and $\bar{A}_{32}$. We determine $\bar{A}_{31}$ by minimizing $\left\|\tau_g^{(6)}\right\|_2$, as a result, it generates a minimum value 8.487×10^{-3} at $\bar{A}_{31} = \frac{-1288}{452405}$, which produces $\bar{A}_{32} = \frac{98209}{2714430} - \frac{\sqrt{5}}{75}$. In the meanwhile, at $\bar{A}_{31} = -\frac{1288}{452405}$, we have $\left\|\tau^{(6)}\right\|_2 \approx 1.626 \times 10^{-3}$ and $\left\|\tau'^{(6)}\right\|_2 \approx 4.599 \times 10^{-3}$. So far, we have preliminarily completed the construction of the ETDRKN(5) method.

4. Implementation of the Trigonometrically-Fitting Technique

Firstly, we look back to the scheme (3), we add $\bar{\chi}_i$ in front of u_n in U and $\tilde{\chi}_i$ in front of $f(t_n, u_n)$ in U_i' and set $\bar{\chi} = (\bar{\chi}_1, \cdots, \bar{\chi}_s)^T$ and $\tilde{\chi} = (\tilde{\chi}_1, \cdots, \tilde{\chi}_s)^T$. The introduction of these two new coefficent vectors is the first step for our trigonometrically-fitting technique.

Rewriting the scheme (3), we get

$$
\begin{aligned}
u_{n+1} &= u_n + hu_n' + \frac{h^2}{2} f(t_n, u_n) + h^3 \sum_{i=1}^{s} \bar{d}_i g\left(t_n + c_i h, U_i, U'_i\right), \\
u_{n+1}' &= u_n' + hf(t_n, u_n) + h^2 \sum_{i=1}^{s} \tilde{d}_i g\left(t_n + c_i h, U_i, U'_i\right), \\
U_i &= \bar{\chi}_i u_n + c_i h u_n' + \frac{1}{2}(c_i h)^2 f(t_n, u_n) + h^3 \sum_{i=1}^{s} \bar{A}_{ij} g\left(t_n + c_i h, U_j, U'_j\right), \\
U_i' &= u_n' + \tilde{\chi}_i c_i h f(t_n, u_n) + h^2 \sum_{i=1}^{s} \tilde{A}_{ij} g\left(t_n + c_i h, U_j, U'_j\right),
\end{aligned}
\tag{22}
$$

The Butcher Tableau for the renewable ETDRKN(5) method is

Table 3: Butcher Tableau for the renewable ETDRKN(5) method.

$$
\begin{array}{c|cc|c|c}
c & \bar{\chi} & \tilde{\chi} & \bar{A} & \tilde{A} \\
\hline
 & & & \bar{d} & \tilde{d_i}
\end{array}
$$

Then, we integrate the exponential terms, $e^{i\lambda t}$ and $e^{-i\lambda t}$ at every stage and $w = \lambda h$ with $\lambda \in \mathbb{R}$, we obtain

$$
e^{\pm i c_i w} = \bar{\chi}_i \pm i c_i w - \frac{1}{2}(c_i w)^2 \mp i w^3 \sum_{i=1}^{3} \bar{A}_{ij} e^{\pm i c_j w}, \ e^{\pm i c_i w} = 1 \pm i \tilde{\chi}_i c_i w - w^2 \sum_{i=1}^{3} \tilde{A}_{ij} e^{\pm i c_j w}.
\tag{23}
$$

The equations corresponding to u and u' are as follows

$$
e^{\pm iw} = 1 \pm iw - \frac{1}{2} w^2 \mp i w^3 \sum_{i=1}^{3} \bar{d}_i e^{\pm i c_i w}, \ e^{\pm iw} = 1 \pm iw - w^2 \sum_{i=1}^{3} \tilde{d}_i e^{\pm i c_i w}.
\tag{24}
$$

The relation

$$
\begin{aligned}
&\cos w = \frac{1}{2}\left(e^{iw} + e^{-iw}\right), \ \sin w = \frac{1}{2i}\left(e^{iw} - e^{-iw}\right), \\
&\cos(c_i w) = \frac{1}{2}\left(e^{i c_i w} + e^{-i c_i w}\right), \ \sin(c_i w) = \frac{1}{2i}\left(e^{i c_i w} - e^{-i c_i w}\right)
\end{aligned}
\tag{25}
$$

are substituted in the equation (25), then we obtain the trigonometric functions in terms of w

$$
\begin{aligned}
&\cos w = 1 - \frac{1}{2}w^2 + w^3 \sum_{i=1}^{3} \bar{d}_i \sin(c_i w),\ \sin w = w - w^3 \sum_{i=1}^{3} \bar{d}_i \cos(c_i w),\\
&\cos w = 1 - w^2 \sum_{i=1}^{3} \tilde{d}_i \cos(c_i w),\ \sin w = w - w^2 \sum_{i=1}^{3} \tilde{d}_i \sin(c_i w),\\
&\cos(c_i w) = 1 - \frac{1}{2}(c_i w)^2 + w^3 \sum_{i=1}^{3} \bar{A}_{ij} \sin(c_j w),\ \sin(c_i w) = c_i w - w^3 \sum_{i=1}^{3} \bar{A}_{ij} \cos(c_j w),\\
&\cos(c_i w) = 1 - w^2 \sum_{i=1}^{3} \tilde{A}_{ij} \cos(c_j w),\ \sin(c_i w) = c_i w - w^2 \sum_{i=1}^{3} \tilde{A}_{ij} \sin(c_j w).
\end{aligned}
\tag{26}
$$

The trigonometrically-fitted coefficients $\bar{A}_{ij}(w)$ and $\tilde{A}_{ij}(w)$ can be obtained by

$$
\begin{aligned}
\bar{A}_{i,i-1}(w) &= \frac{\cos(c_j w) - 1 + \frac{1}{2}(c_i w)^2 - w^3 \sum\limits_{j=1}^{i-2} \bar{A}_{ij} \sin(c_j w)}{w^3 \sin(c_{i-1} w)},\\
\tilde{A}_{i,i-1}(w) &= \frac{1 - \cos(c_j w) - w^2 \sum\limits_{j=1}^{i-2} \tilde{A}_{ij} \cos(c_j w)}{w^2 \cos(c_{i-1} w)}.
\end{aligned}
\tag{27}
$$

Then $\bar{\chi}_i(w)$ and $\tilde{\chi}_i(w)$ are determined on the coefficients $\bar{A}_{i,i-1}(w)$ and $\tilde{A}_{i,i-1}(w)$ through

$$
\begin{aligned}
\bar{\chi}_i(w) &= \cos(c_i w) + \frac{1}{2}(c_i w)^2 - w^3 \sum_{i=1}^{3} \bar{A}_{ij} \sin(c_j w),\\
\tilde{A}_{i,i-1}(w) &= \frac{\sin(c_i w) + w^2 \sum\limits_{i=1}^{3} \tilde{A}_{ij} \sin(c_j w)}{c_i w}.
\end{aligned}
\tag{28}
$$

Modifying the equations (27,28), we obtain the trigonometrically-fitted coefficients $\bar{A}_{ij}(w)$, $\tilde{A}_{ij}(w)$, $\bar{\chi}_i(w)$ and $\tilde{\chi}_i(w)$

$$
\begin{aligned}
&\bar{A}_{21}(w) = \frac{c_2 w - \sin(c_2 w)}{w^3},\ \bar{A}_{32}(w) = \frac{c_3 w - \sin(c_3 w) - \bar{A}_{31} w^3}{w^3 \cos(c_2 w)},\\
&\tilde{A}_{21}(w) = \frac{1 - \cos(c_2 w)}{w^2},\ \tilde{A}_{32}(w) = \frac{1 - \cos(c_3 w) - \tilde{A}_{31} w^2}{w^2},\\
&\bar{\chi}_2(w) = \cos(c_2 w) + \frac{1}{2}(c_2 w)^2,\ \bar{\chi}_3(w) = \cos(c_3 w) + \frac{1}{2}(c_3 w)^2 - \bar{A}_{32} \sin(c_2 w),\\
&\tilde{\chi}_2(w) = \frac{\sin(c_3 w)}{c_3 w},\ \tilde{\chi}_3(w) = \frac{\sin(c_3 w) + w^2 \tilde{A}_{32} \sin(c_2 w)}{c_3 w}.
\end{aligned}
\tag{29}
$$

Then, by substituting all the coefficients (20) of the ETDRKN(5) method into the equations (29) and employing the eighth-order Taylor series expansion, we compute the frequency-dependent coefficients for $\bar{A}_{ij}(w)$, $\tilde{A}_{ij}(w)$, $\bar{\chi}_i(w)$ and $\tilde{\chi}_i(w)$ (see eqs 59 in Appendices).

As a result, we conduct a novel trigonometrically-fitted explicit two-derivative Runge-Kutta-Nyström with the three-stage and fifth-order (TFETDRKN(5)) method. The Butcher Tableau for the TFETDRKN(5) method is

Table 4: Butcher Tableau for the TFETDRKN(5) method.

$$
\begin{array}{c|cc|ccc|ccc}
c_1(w) & 0 & 0 & 0 & 0 & 0 & 0 & 0 & 0 \\
c_2(w) & \bar{\chi}_2(w) & \tilde{\chi}_2(w) & \bar{A}_{21}(w) & 0 & 0 & \tilde{A}_{21}(w) & 0 & 0 \\
c_3(w) & \bar{\chi}_3(w) & \tilde{\chi}_3(w) & \bar{A}_{31}(w) & \bar{A}_{32}(w) & 0 & \tilde{A}_{31}(w) & \tilde{A}_{32}(w) & 0 \\
\hline
 & & & \bar{d}_1(w) & \bar{d}_2(w) & \bar{d}_3(w) & \tilde{d}_1(w) & \tilde{d}_2(w) & \tilde{d}_3(w)
\end{array}
$$

Observe that as w approaches zero, all trigonometrically-fitted coefficients derived above for the TFETDRKN(5) method converge to the original constant coefficients for the ETDRKN(5) method.

Remark 1. *The addition of vectors $\bar{\chi}$ and $\tilde{\chi}$, and the generation of trigonometrically-fitted coefficients is to make the proposed method more accurate in solving second-order ODEs with periodic solutions, which is also the key point of this paper.*

5. Stability Analysis

5.1. Stability matrix

For testing the stability properties of the TFETDRKN(5) method, we use the homogeneous test equation ([17])

$$u'' = -\mu^2 u, \ \mu > 0 \tag{30}$$

where μ is the natural frequency. By applying the scheme (3) to the test equation (30), we obtain

$$\begin{pmatrix} u_{n+1} \\ hu'_{n+1} \end{pmatrix} = N\left(z^2; w\right) \begin{pmatrix} u_n \\ hu'_n \end{pmatrix}, \tag{31}$$

where

$$N\left(z^2; w\right) = \begin{pmatrix} 1 - \frac{z^2}{2} + z^4 \bar{d}(w)^T \left(I + z^2 \tilde{A}(w)\right)^{-1} \tilde{\chi}(w)\, ce & 1 - z^2 \bar{d}(w)^T \left(I + z^2 \tilde{A}(w)\right)^{-1} e \\ -z^2 + z^4 \tilde{d}(w)^T \left(I + z^2 \tilde{A}(w)\right)^{-1} \tilde{\chi}(w)\, ce & 1 - z^2 \tilde{d}(w)^T \left(I + z^2 \tilde{A}(w)\right)^{-1} e \end{pmatrix}, \ z = \mu h \tag{32}$$

is called the stability matrix of the TFETDRKN(5) method.

Remark 2. *λ in $w = \lambda h$ is called fitted frequency, while μ in $z = \mu h$ is called natural frequecny. For the trigonometrically-fitted methods applied to problems like* (1)*, the fitted frequency of methods generally differs from the natural frequency of the theoretical solution. However, for the linear oscillator $u''(t)+\lambda^2 u(t) = 0$, the method's fitted frequency matches the natural frequency of the theoretical solution [22]. So we will conduct the stability analysis considering two cases, $\lambda = \mu$ and $\lambda \neq \mu$.*

5.2. Dispersion and dissipation error analysis

Stability behavior of the numerical solution depends on eigenvalues $\xi_i (i = 1, 2)$ of the stability matrix (32). Eliminating u'_{n+1} and u'_n from the equations (31) by replacing the subscript 0 by 1 and 1 by 2 yields the difference equation

$$u_2 - \operatorname{tr}(N)\, u_1 + \det(N)\, u_0 = 0. \tag{33}$$

Accordingly, we obtain the characteristic polynomial $\sigma(z, w; \xi)$

$$\sigma(z, w; \xi) = \xi^2 - \operatorname{tr}(N)\, \xi + \det(N) = 0, \tag{34}$$

where $\operatorname{tr}(N)$ and $\det(N)$ are the trace and the determinant of the stability matrix (32), ξ_1 and ξ_2 are

$$\xi_1 = \frac{\operatorname{tr}(N) - \sqrt{\operatorname{tr}^2(N) - 4\det(N)}}{2},\ \xi_2 = \frac{\operatorname{tr}(N) + \sqrt{\operatorname{tr}^2(N) - 4\det(N)}}{2}. \tag{35}$$

Definition 1 ([17])**.** *For the characteristic polynomial (34), we set the ratio $\kappa = \frac{\lambda}{\mu}$, then introduce two quantities*

$$\phi(z; \kappa) = z - \arccos\left(\frac{\operatorname{tr}(N)}{2\sqrt{\det(N)}}\right),\ \psi(z; \kappa) = 1 - \sqrt{\det(N)}, \tag{36}$$

which are denoted as the dispersion error and the dissipation error respectively. TFETDRKN(5) method is dispersive and dissipative of order s and order k respectively, if

$$\phi(z; \kappa) = O\left(z^{s+1}\right),\ \psi(z; \kappa) = O\left(z^{k+1}\right). \tag{37}$$

And the necessary and sufficient condition for the TFETDRKN(5) method is dispersive and dissipative of order s and order k respectively, is that the expression $\gamma(z; \kappa)$ and $\vartheta(z; \kappa)$ satisfies [23]

$$\gamma(z; \kappa) = \operatorname{tr}(N) - 2\sqrt{\det(N)}\cos(z) = O\left(z^{s+2}\right),\ \vartheta(z; \kappa) = \det(N) - 1 = O\left(z^{k+1}\right). \tag{38}$$

By calculating via Maple, for $\lambda = \mu$, we have

$$\gamma(w) = \frac{1}{4}w^4 + \left(-\frac{4}{45} + \frac{\sqrt{5}}{120}\right) w^6 + O\left(w^8\right),\ \vartheta(w) = -\frac{1}{6}w^4 + \left(-\frac{\sqrt{5}}{160} + \frac{1}{160}\right) w^6 + O\left(w^8\right), \tag{39}$$

for $\lambda \neq \mu$, we have

$$\begin{aligned} \gamma(z;\kappa) &= \frac{1}{4}z^4 + \frac{1}{7200}((12\sqrt{5}+20)\kappa^2 + 33\sqrt{5} - 645)z^6 + O\left(z^8\right), \\ \vartheta(z;\kappa) &= -\frac{1}{6}z^4 - \frac{\sqrt{5}}{7200}((4\sqrt{5}+12)\kappa^2 - 13\sqrt{5} + 33)z^6 + O\left(z^8\right). \end{aligned} \tag{40}$$

So the TFETDRKN(5) method is dispersive of order two and dissipative of order three from conditions (38).

5.3. Stability properties and regions

In this subsection, we study the stability properties and regions of the TFETDRKN(5) method comprehensively to predict its efficiency region and range corresponding to different step sizes for two cases, $\lambda = \mu$ and $\lambda \neq \mu$.

5.3.1. For the case of same frequency

Definition 2 ([14]). *We define the stability region for the TFETDRKN(5) method as follows:*

$$R_S = \{w : |\xi_i| < 1, i = 1, 2\},$$

where $\xi_i\,(i = 1, 2)$ are the eigenvalues of $N\left(w^2\right)$.

The stability regions for different ranges of the TFETDRKN(5) method with $\lambda = \mu$ are shown in Figs. 1-6. The stability region for w is the intersection region of stability region for w_1 and w_2. Note that the stability region still exists when w is relatively larger, but the detailed research in such case is not very meaningful because in numerical simulations, the step size h usually takes at least one decimal place and the frequency λ will not be very large, so w will not be so lager.

Fig. 7 and Figs. 8, 9 show the distribution relationship of ξ, ξ_1 and ξ_2 versus w. Moreover, the curves of $\xi_i, abs(\xi_i)(i = 1, 2)$ and zeros of denominator are also shown intuitively. According to such three figures, the approximate w range that meets Here is your expression with quotation marks added (using proper LaTeX quoting): latex“$|\xi_i| < 1, i = 1, 2$” can be concluded.

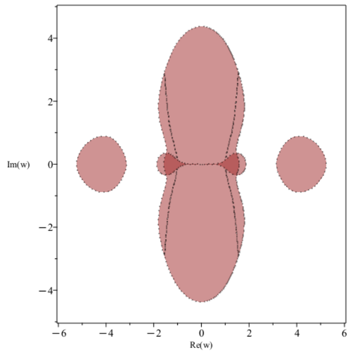

Figure 1: Stability region for the real part of $w \in [-6, 6]$.

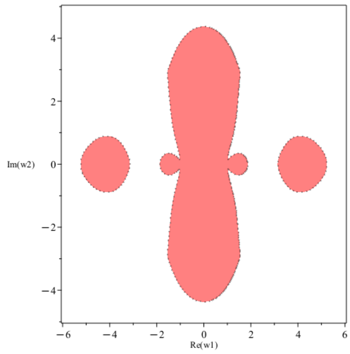

Figure 2: Partial stability region for the real part of $w_1 \in [-6, 6]$.

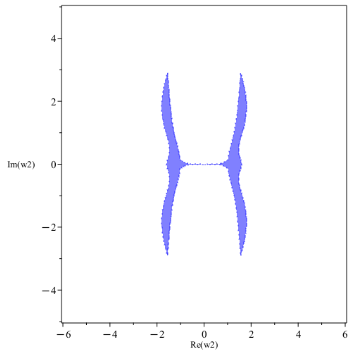

Figure 3: Partial stability region for the real part of $w_2 \in [-6, 6]$.

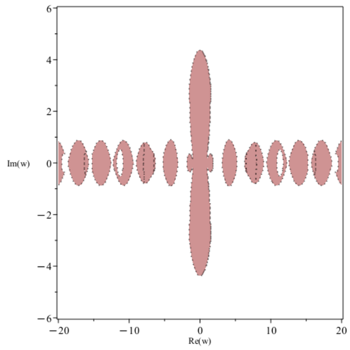

Figure 4: Stability region for the real part of $w \in [-20, 20]$

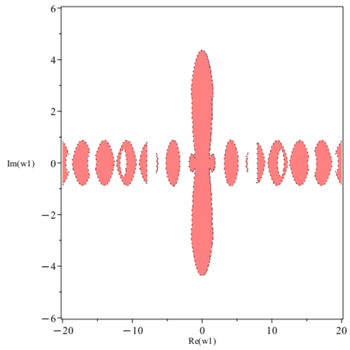

Figure 5: Partial stability region for the real part of $w_1 \in [-20, 20]$.

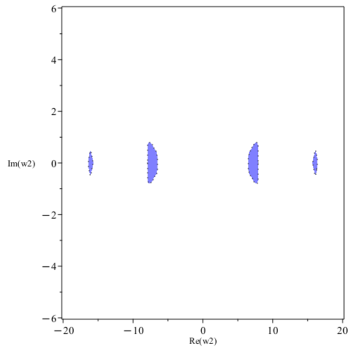

Figure 6: Partial stability region for the real part of $w_2 \in [-20, 20]$.

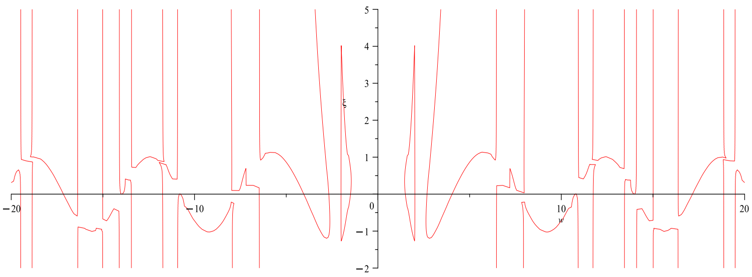

Figure 7: Stability property of characteristic polynomial for ξ against w.

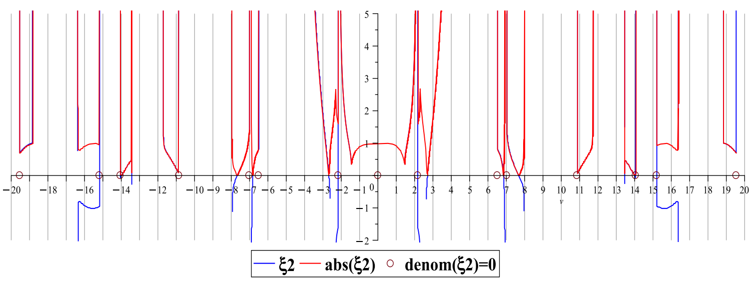

Figure 8: Stability property of characteristic polynomial for ξ_1 against w.

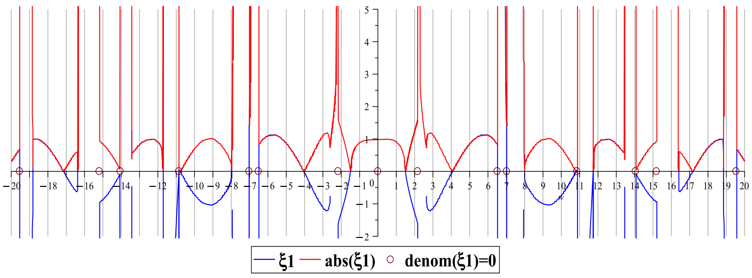

Figure 9: Stability property of characteristic polynomial for ξ_2 against w.

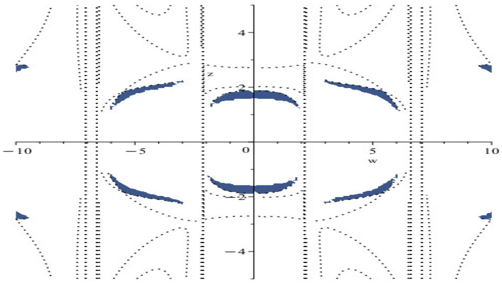

Figure 10: Periodicity stability region for z against w.

Definition 3 ([14]). *An interval $I = (-\tilde{w}, 0)$ is said to be an interval of stability of the TFETDRKN(5) method if for all $\tilde{w} \in I$, it is $|\xi_{1,2}| < 1$.*

The performance of the range of w when ξ is between -1 and 1 is worth studying, then by calculation via Maple, we obtain the interval of stability for ξ_1 is $(-1.866, 0)$ and for ξ_2 is $(-1.588, 0)$, so the interval of stability for the TFETDRKN(5) method is $(-1.588, 0)$.

5.3.2. For the case of different frequency

Definition 4 ([17]). *For the TFETDRKN(5) method with the stability matrix $N\left(z^2; w\right)$ and its eigenvalues, $\xi_i\,(i = 1, 2)$, the region in complex plane*

$$R_P = \{(w, z) : |\xi_i| < 1, i = 1, 2\}$$

is called the periodicity region of the TFETDRKN(5) method.

The periodicity region of the TFETDRKN(5) method with $\lambda \neq \mu$ is depicted in Fig. 10. For similar reason to the stability regions mentioned in the subsection 5.3.1, we are more focused on the distribution when w and z take relatively smaller values.

Figs. 11-14 illustrate the stability property of characteristic polynomial (34) for different w, z range and contour on different value of ξ. Note that four different w, z ranges of four figures can fit the frequency, λ, μ and step size, h of most experiments, so we can obtain the approximate w, z regions that meet "$|\xi_i| < 1, i = 1, 2$".

6. Algebraic Order Analysis

In order to derive a general formula for the higher-order derivatives of the theoretical solution of the problem (1), we propose expressing the theoretical solution, $u\,(t)$ at $t = t_0$

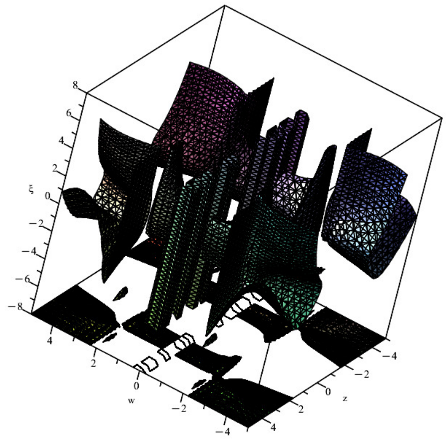

Figure 11: Stability property of characteristic polynomial with $w, z \in [-5, 5]$ and contour on $\xi = -8$.

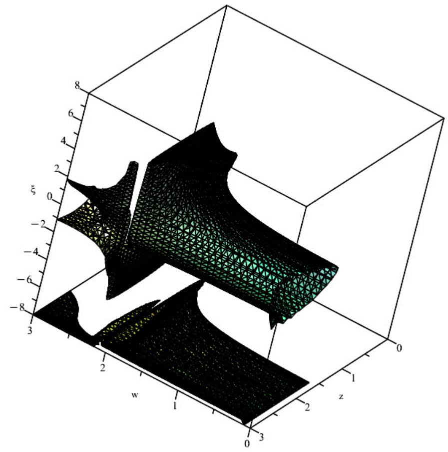

Figure 12: Stability property of characteristic polynomial with $w, z \in [0, 3]$ and contour on $\xi = -8$.

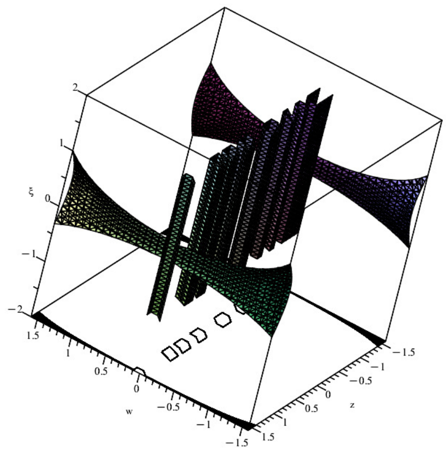

Figure 13: Stability property of characteristic polynomial with $w, z \in [-1.588, 1.588]$ and contour on $\xi = -2$.

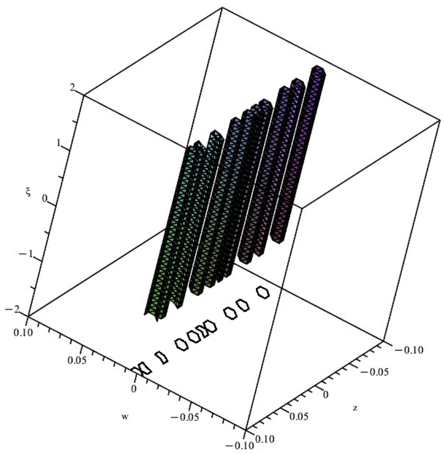

Figure 14: Stability property of characteristic polynomial with $w, z \in [-0.1, 0.1]$ and contour on $\xi = -2$.

from first to seventh derivatives

$$
\begin{aligned}
u^{(1)} =& z, u^{(2)} = f, u^{(3)} = g, u^{(4)} = g_u z + g_z f, u^{(5)} = g_{uu} z^2 + 2 g_{uz} f z + g_u f + g_{zz} f^2 + g_z g, \\
u^{(6)} =& g_{uuu} z^3 + 3 \left(g_{uuz} f z^2 + g_{uu} f z + g_{uzz} f^2 z + g_{uz} g z + g_{uz} f^2 + g_{zz} g f \right) + g_u g \\
& + g_{zzz} f^3 + g_z \left(g_u z + g_z f \right), \\
u^{(7)} =& 12 \left(g_{uzz} g f z + g_{uuz} f^2 z \right) + 10 g_{uz} g f + 6 \left(g_{uuu} f z^2 + g_{uuzz} f^2 z^2 + g_{uuz} g z^2 + g_{zzz} g f^2 + g_{uzz} f^3 \right) \\
& + 4 \left(g_{uu} g z + g_{uzzz} f^3 z + g_{uz} g_u z^2 + g_{uz} g_z f z + g_{zz} g_u f z + g_{zz} g_z f^2 + g_{uuuz} f z^3 \right) \\
& + 3 \left(g_{uu} f^2 + g_{zz} g^2 \right) + g_z \left(g_{uu} z^2 + 2 g_{uz} f z + g_u f + g_{zz} f^2 + g_z g \right) \\
& + {}'_u \left(g_u z + g_z f \right) + g_{uuuu} z^4 + g_{zzzz} f^4.
\end{aligned}
\tag{41}
$$

Then we demonstrate the LTEs for u and u' generated by the ETDRKN(5) method. The Taylor series expansion is applied over h to the theoretical solution $u(t_n + h)$, its derivative $u'(t_n + h)$, the numerical solution u_{n+1}, and its derivative u'_{n+1}. For the ETDRKN(5) method, the LTEs at t_{n+1} for both the theoretical and numerical solutions, along with their respective derivatives, are given as follows

$$\begin{aligned}
LTE_{no\,fitted}(u) &= u_{n+1} - u\left(t_n + h\right) = \left(\frac{1}{2400}\left(\frac{5}{3} - \sqrt{5}\right)\left(g_z^2 + g_z g_u z + 4 g_u g\right)\right) \cdot w^6 + O\left(w^7\right), \\
LTE_{no\,fitted}(u') &= u'_{n+1} - u'\left(t_n + h\right) \\
&= \left(\frac{1}{1200}\left(\sqrt{5} - \frac{5}{3}\right)\left(g_{uz} g_z - \frac{1}{2} g_{uu}\right) z^2 \right. \\
&\quad + \left(\frac{\sqrt{5}}{325731600}\left(271443 g_{zz} g_z f - 723848 g_{uu} g - 1033931 {g_z}^2\right) - 452405 g_{zz} g_z f + 1925540 {g_z}^2\right) z \\
&\quad + \frac{\sqrt{5}}{651463200}\left(271443 g_{zz} g_z f^2 - 1447696 g_{uz} g f - 2339305 g_z g_z f - 271443 {g_z}^2 g\right) \\
&\quad \left. - \frac{1}{1440}\left(g_{zz} f^2 - \frac{860697}{90481} g_z f - g_z g\right) g_z \right) \cdot w^6 + O\left(w^7\right).
\end{aligned} \tag{42}$$

LTEs for u and u' of the ETDRKN(5) method up to h^5 vanish, so the ETDRKN(5) method is algebraic of order 5.

7. Numerical Experiments and Results

We solve problems (1) with the theoretical solution generated by the following linear space

$$\left\{1, t, t^2, \cos(\lambda t), \sin(\lambda t)\right\} \tag{43}$$

We use several typical second-order ODEs with periodic solutions (43) to demonstrate the effectiveness and accuracy of the TFETDRKN(5) method. We conduct the experiments testing and get the numerical results by plotting the tables and figures comparing other selected existing methods in terms of the maximum global truncation error, the number of function evaluations and CPU time in seconds. The numerical methods used for comparison are

- **TFTDRKN3s5**: Existing trigonometrically-fitted two-derivative Runge-Kutta-Nyström method of three stage fifth-order [17].
- **STDRKN5(3)**: Existing efficient two-derivative Runge-Kutta-Nyström Method of three stage fifth-order [18].
- **PFAFRKN6-6ER**: Existing optimized sixth-order explicit Runge-Kutta-Nyström Method to solve oscillating systems [24].
- **TFIRKN5**: Existing fifth-order improved Runge-Kutta-Nyström Method using trigonometrically [25].

Several notations used are

- h: step size
- B: endpoint of value t
- Time(s): CPU time in seconds
- NFE: number of function evaluation
- $MGTE$: maximum global truncation error from numerical experiments
- $4.084364(-16)$: 4.084364×10^{-16}

The maximum global truncation error (MGTE) is defined by

$$MGTE = \max |u_n - u(t_n)|,$$

where u_n is numerical solution and $u(t_n)$ is theoretical solution at endpoint, $t_n = B$.

Experiment 1: Consider the homogeneous problem [26]

$$\begin{cases} u''(t) = -64u(t), \ t \in [0, 100], \\ u(0) = -\dfrac{1}{4}, \ u'(0) = -\dfrac{1}{2}, \end{cases}$$

with the theoretical solution:

$$u(t) = -\frac{1}{16}\sin(8t) + \frac{1}{4}\cos(8t).$$

Natural frequency, $\lambda = 8$.

Experiment 2: Consider the linear second-order problem [27]

$$\begin{cases} u''(t) = -u(t) + 2, \ t \in [0, 100], \\ u(0) = 0, \ u'(0) = 1, \end{cases}$$

with the theoretical solution:

$$u(t) = 2(1 - \cos(t)) + \sin(t).$$

Fitted frequency, $\lambda = 1$.

Experiment 3: Consider one typical stiff problem [28]

$$\begin{cases} u''(t) = \begin{pmatrix} -\frac{1}{2}(\beta^2 + 1) & -\frac{1}{2}(\beta^2 - 1) \\ -\frac{1}{2}(\beta^2 - 1) & -\frac{1}{2}(\beta^2 + 1) \end{pmatrix} u(t), \ t \in [0, 100], \\ u(0) = (1, -1)^T, \ u'(0) = (1, -1)^T, \end{cases}$$

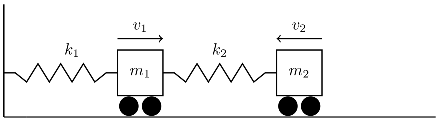

Figure 15: Experiment 4

with the theoretical solution:

$$u\left(t\right)=\left(\cos\left(t\right)+\sin\left(t\right),\ -\left(\cos\left(t\right)+\sin\left(t\right)\right)\right)^{T}.$$

Fitted frequency, $\lambda=1$. We select $\beta=2$, 10^{2} and 10^{4} to test this problem, respectively.

Experiment 4 (Fig. 15): Consider one undamped mass-spring system [29]

$$\begin{cases}\begin{pmatrix} m_1 & 0 \\ 0 & m_2 \end{pmatrix} u''\left(t\right)=\begin{pmatrix} -\left(k_1+k_2\right) & k_2 \\ k_2 & -k_2 \end{pmatrix} u\left(t\right),\ t\in[0,100], \\ u\left(0\right)=\left(0,0\right)^{T},\ u'\left(0\right)=\left(3,-2\right)^{T}. \end{cases} \tag{44}$$

We set $m_1=\frac{13}{3}\text{kg}$, $m_2=5\text{kg}$, $k_1=1\text{N}\cdot\text{m}^{-1}$, $k_2=2\text{N}\cdot\text{m}^{-1}$, so the theoretical solution is

$$u\left(t\right)=\left(3\sin\left(t\right),\ -2\sin\left(t\right)\right)^{T}. \tag{45}$$

Fitted frequency, $\lambda=1$.

Experiment 5 (Fig. 16) : Consider another undamped mass-spring system [29]

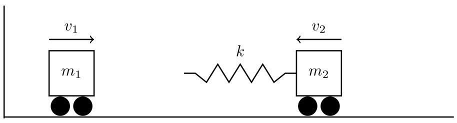

Figure 16: Experiment 5

$$\begin{cases}\begin{pmatrix} m_1 & 0 \\ 0 & m_2 \end{pmatrix} u''\left(t\right)=\begin{pmatrix} -k & k \\ k & -k \end{pmatrix} u\left(t\right),\ t\in[0,100], \\ u\left(0\right)=\left(0,0\right)^{T},\ u'\left(0\right)=\left(10,-1\right)^{T}. \end{cases} \tag{46}$$

We set $m_1=8\text{kg}$, $m_2=7\text{kg}$,$k_1=56\text{N}\cdot\text{m}^{-1}$, so the theoretical solution is

$$u\left(t\right)=\left(\frac{73}{15}t+\frac{77\sqrt{15}}{225}\sin\left(\sqrt{15}t\right),\ \frac{73}{15}t-\frac{88\sqrt{15}}{225}\sin\left(\sqrt{15}t\right)\right)^{T}. \tag{47}$$

Fitted frequency, $\lambda=\sqrt{15}$. Let $t=0$ be the moment when the two cars meet. Then two cars begin to compress the spring till the spring's elastic potential energy reaches its maximum critical point, the spring stretches and becomes longer, and finally the two cars separate (not considering any car hitting the wall).

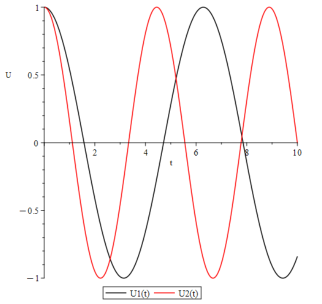

Figure 17: RK4 method for experiment 8 with $h = 10^{-5}$ and $B = 10$.

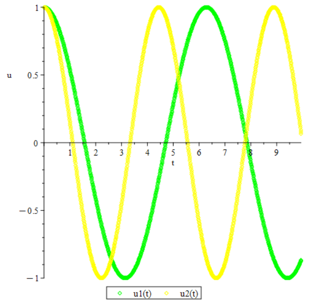

Figure 18: TFETDRKN(5) method for experiment 8 with $h = 10^{-3}$ and $B = 10$.

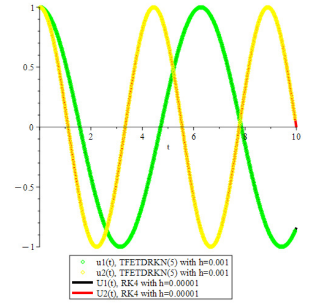

Figure 19: Numerical simulation for experiment 8 with $h = 10^{-3}$ and $B = 10$.

Experiment 6: Consider the "two coupled oscillators with different frequencies" system [30]

$$\begin{cases} u''(t) = \begin{pmatrix} -1 & 0 \\ 0 & -2 \end{pmatrix} u(t) + \begin{pmatrix} 2\varepsilon u_1(t)\, u_2(t) \\ \varepsilon\left({u_1}^2(t) + 4{u_2}^3(t)\right) \end{pmatrix},\ t \in [0,5], \\ u(0) = (1,1)^T,\ u'(0) = (0,0)^T. \end{cases} \tag{48}$$

The use of a perturbation method yields the first-order fitted frequencies [31]

$$\lambda_{u_1} = 1 \cdot \lambda_{u_2} = \sqrt{2} - \frac{3\varepsilon}{\sqrt{2}}. \tag{49}$$

We set $\varepsilon = 10^{-4}$. As we are unable to obtain the theoretical solution for experiment 8, we use the numerical solution generated by the classical fourth-order Runge-Kutta method with step size, $h = 10^{-5}$ as its theoretical solution and compare it with other comparative methods. Figs. 17, 18, 19 display the numerical simulation with $B = 10$.

8. Tables and Graphs of Numerical Results

Table 5: Experiment 1.

h	METHOD	MGTE	NFE	Time(s)
0.025	TFETDRKN(5)	4.084364(-16)	12000	0.519
	TFTDRKN3s5	1.802952(-13)	12000	0.539
	STDRKN5	1.562715(-5)	12000	0.587
	PFAFRKN6-6ER	5.960929(-13)	24000	0.719
	TFIRKN5	1.912294(-4)	32000	0.632
0.020	TFETDRKN(5)	1.144546(-17)	15000	0.595
	TFTDRKN3s5	1.934776(-14)	15000	0.632
	STDRKN5	5.115801(-6)	15000	0.749
	PFAFRKN6-6ER	1.039706(-13)	30000	0.856
	TFIRKN5	6.171445(-5)	40000	0.754
0.015	TFETDRKN(5)	1.142831(-19)	20000	0.756
	TFTDRKN3s5	1.089515(-15)	20000	0.932
	STDRKN5	1.214425(-6)	20000	0.938
	PFAFRKN6-6ER	1.140415(-14)	40000	1.145
	TFIRKN5	1.450237(-5)	53333	1.014
0.010	TFETDRKN(5)	1.737694(-22)	30000	1.250
	TFTDRKN3s5	7.568127(-17)	30000	1.260
	STDRKN5	1.599277(-7)	30000	1.309
	PFAFRKN6-6ER	5.498041(-16)	60000	1.769
	TFIRKN5	1.895651(-6)	80000	1.509
0.005	TFETDRKN(5)	2.648241(-27)	60000	2.447
	TFTDRKN3s5	1.847588(-20)	60000	2.601
	STDRKN5	4.996194(-9)	60000	2.688
	PFAFRKN6-6ER	3.887940(-18)	120000	3.390
	TFIRKN5	5.894875(-8)	160000	3.072

Table 6: Experiment 2.

h	METHOD	MGTE	NFE	Time(s)
0.025	TFETDRKN(5)	1.529179(-30)	12000	0.426
	TFTDRKN3s5	1.790330(-22)	12000	0.470
	STDRKN5	5.168409(-10)	12000	0.467
	PFAFRKN6-6ER	1.998151(-18)	24000	0.675
	TFIRKN5	6.103274(-9)	32000	0.595
0.020	TFETDRKN(5)	4.303836(-32)	15000	0.517
	TFTDRKN3s5	1.922284(-23)	15000	0.593
	STDRKN5	1.693915(-10)	15000	0.594
	PFAFRKN6-6ER	4.654337(-19)	30000	0.794
	TFIRKN5	1.999367(-9)	40000	0.798
0.015	TFETDRKN(5)	4.313117(-34)	20000	0.768
	TFTDRKN3s5	1.082461(-24)	20000	0.771
	STDRKN5	4.016910(-11)	20000	0.856
	PFAFRKN6-6ER	7.367519(-20)	40000	1.083
	TFIRKN5	4.739915(-10)	53333	1.087
0.010	TFETDRKN(5)	6.566061(-37)	30000	1.022
	TFTDRKN3s5	1.877093(-26)	30000	1.079
	STDRKN5	5.295473(-12)	30000	1.142
	PFAFRKN6-6ER	5.770130(-21)	60000	1.547
	TFIRKN5	6.245495(-11)	80000	1.381
0.005	TFETDRKN(5)	1.001838(-41)	60000	2.075
	TFTDRKN3s5	1.833039(-29)	60000	2.340
	STDRKN5	1.655133(-13)	60000	2.502
	PFAFRKN6-6ER	8.089612(-23)	120000	3.285
	TFIRKN5	1.951468(-12)	160000	3.022

Table 7: Experiment 3.

h	METHOD	MGTE	NFE	Time(s)
0.1	TFETDRKN(5)	4.256602(-21)	3000	1.194
	TFTDRKN3s5	1.213163(-16)	3000	1.126
	STDRKN5(3)	3.294553(-7)	3000	1.167
	PFAFRKN6-6ER	1.998695(-14)	6000	1.296
	TFIRKN5	3.907366(-6)	8000	1.202
0.05	TFETDRKN(5)	6.479610(-26)	6000	2.293
	TFTDRKN3s5	1.184842(-19)	6000	2.369
	STDRKN5(3)	1.029791(-8)	6000	2.433
	PFAFRKN6-6ER	1.175856(-16)	12000	2.609
	TFIRKN5	1.213642(-7)	16000	2.288
0.025	TFETDRKN(5)	9.881954(-31)	12000	4.717
	TFTDRKN3s5	1.156993(-22)	12000	4.636
	STDRKN5(3)	3.217851(-10)	12000	4.643
	PFAFRKN6-6ER	1.187549(-18)	24000	5.514
	TFIRKN5	3.787327(-9)	32000	4.811
0.0125	TFETDRKN(5)	1.507622(-35)	24000	9.141
	TFTDRKN3s5	1.129826(-25)	24000	9.395
	STDRKN5(3)	1.005527(-11)	24000	8.970
	PFAFRKN6-6ER	1.701612(-20)	48000	10.141
	TFIRKN5	1.183191(-10)	64000	9.670
0.00625	TFETDRKN(5)	2.300318(-40)	48000	18.993
	TFTDRKN3s5	1.103319(-28)	48000	18.874
	STDRKN5(3)	3.142220(-13)	48000	18.869
	PFAFRKN6-6ER	2.679244(-22)	96000	20.045
	TFIRKN5	3.697447(-12)	128000	19.941

Table 8: Experiment 4.

h	METHOD	MGTE	NFE	Time(s)
	TFETDRKN(5)	8.759277(-21)	6000	0.349
	TFTDRKN3s5	2.498800(-16)	6000	0.403
0.1	STDRKN5(3)	7.048727(-7)	6000	0.387
	PFAFRKN6-6ER	7.562986(-14)	12000	0.594
	TFIRKN5	8.102380(-6)	16000	0.504
	TFETDRKN(5)	1.334936(-25)	12000	0.829
	TFTDRKN3s5	2.440855(-19)	12000	0.922
0.05	STDRKN5(3)	2.202624(-8)	12000	1.075
	PFAFRKN6-6ER	4.602406(-16)	24000	1.146
	TFIRKN5	2.514992(-7)	32000	0.951
	TFETDRKN(5)	2.036323(-30)	24000	1.611
	TFTDRKN3s5	2.384085(-22)	24000	1.700
0.025	STDRKN5(3)	6.882515(-10)	24000	1.937
	PFAFRKN6-6ER	4.373250(-18)	48000	2.187
	TFIRKN5	7.849286(-9)	64000	2.040
	TFETDRKN(5)	3.106811(-35)	48000	3.079
	TFTDRKN3s5	2.328292(-25)	48000	3.517
0.0125	STDRKN5(3)	2.150783(-11)	48000	3.398
	PFAFRKN6-6ER	5.732428(-20)	96000	4.433
	TFIRKN5	2.452453(-10)	128000	4.163
	TFETDRKN(5)	4.740479(-40)	96000	6.506
	TFTDRKN3s5	2.273722(-28)	96000	6.956
0.00625	STDRKN5(3)	6.721108(-13)	96000	6.572
	PFAFRKN6-6ER	8.526926(-22)	192000	9.334
	TFIRKN5	7.664112(-12)	256000	8.725

Table 9: Experiment 5.

h	METHOD	MGTE	NFE	Time(s)
0.1	TFETDRKN(5)	4.622706(-11)	6000	0.366
	TFTDRKN3s5	3.732735(-10)	6000	0.378
	STDRKN5(3)	1.207628(-3)	6000	0.449
	PFAFRKN6-6ER	1.599813(-9)	12000	0.514
	TFIRKN5	1.614405(-2)	16000	0.450
0.05	TFETDRKN(5)	6.864049(-16)	12000	0.725
	TFTDRKN3s5	3.684791(-13)	12000	0.789
	STDRKN5(3)	3.769888(-5)	12000	0.894
	PFAFRKN6-6ER	6.523295(-12)	24000	1.134
	TFIRKN5	4.568589(-4)	32000	1.355
0.025	TFETDRKN(5)	1.039558(-20)	24000	1.416
	TFTDRKN3s5	3.597012(-16)	24000	1.495
	STDRKN5(3)	1.177672(-6)	24000	1.769
	PFAFRKN6-6ER	2.986460(-14)	48000	2.146
	TFIRKN5	1.388403(-5)	64000	1.829
0.0125	TFETDRKN(5)	1.582759(-25)	48000	2.941
	TFTDRKN3s5	3.512880(-19)	48000	3.156
	STDRKN5(3)	3.680162(-8)	48000	3.282
	PFAFRKN6-6ER	1.852287(-16)	96000	4.082
	TFIRKN5	4.308162(-7)	128000	3.997
0.00625	TFETDRKN(5)	2.414464(-30)	96000	6.112
	TFTDRKN3s5	3.430763(-22)	96000	6.285
	STDRKN5(3)	1.149993(-9)	96000	6.428
	PFAFRKN6-6ER	1.795039(-18)	192000	8.336
	TFIRKN5	1.344022(-8)	256000	7.670

Table 10: Experiment 6

h	METHOD	MGTE	NFE	Time(s)
0.1	TFETDRKN(5)	5.677404(-8)	300	0.015
	TFTDRKN3s5	7.829360(-9)	300	0.018
	STDRKN5(3)	8.618116(-8)	300	0.020
	PFAFRKN6-6ER	3.727733(-12)	600	0.074
	TFIRKN5	1.424941(-1)	800	0.023
0.05	TFETDRKN(5)	1.717588(-9)	600	0.037
	TFTDRKN3s5	2.441104(-10)	600	0.039
	STDRKN5(3)	2.677502(-9)	600	0.084
	PFAFRKN6-6ER	2.800499(-14)	1200	0.105
	TFIRKN5	7.075647(-2)	1600	0.047
0.025	TFETDRKN(5)	5.289724(-11)	1200	0.088
	TFTDRKN3s5	7.621687(-12)	1200	0.074
	STDRKN5(3)	8.348074(-11)	1200	0.121
	PFAFRKN6-6ER	6.531133(-16)	2400	0.148
	TFIRKN5	3.528249(-2)	3200	0.135
0.0125	TFETDRKN(5)	1.641778(-12)	2400	0.134
	TFTDRKN3s5	2.380660(-13)	2400	0.167
	STDRKN5(3)	2.605529(-12)	2400	0.208
	PFAFRKN6-6ER	4.074754(-17)	4800	0.262
	TFIRKN5	1.759057(-2)	6400	0.234
0.00625	TFETDRKN(5)	5.113543(-14)	4800	0.350
	TFTDRKN3s5	7.437993(-15)	4800	0.394
	STDRKN5(3)	8.136990(-14)	4800	0.376
	PFAFRKN6-6ER	2.546304(-18)	9600	0.523
	TFIRKN5	8.750423(-3)	12800	0.382

The following tables and figures present the numerical results, each demonstrating the performance of five different methods, with the exception of experiment 6.The model of computer for experiments is Lenovo ideapad 330 Intel Core i5-8050U (1.8GHz). Evidently, for the MGTE of the first seven experiments, the TFETDRKN(5) method significantly outperforms other existing methods. This is attributable not only to the incorporation of trigonometrically-fitted terms, $\bar{\chi}$ and $\tilde{\chi}$, but also to the application of the trigonometrically-fitting technique, as outlined in section 4, to a larger set of coefficients (compared to conventional trigonometrically-fitting techniques in existing literature), rendering them frequency-dependent due to the inclusion of these terms. Furthermore, our proposed method is specifically tailored for solving special second-order ODEs with periodic solutions like (1).

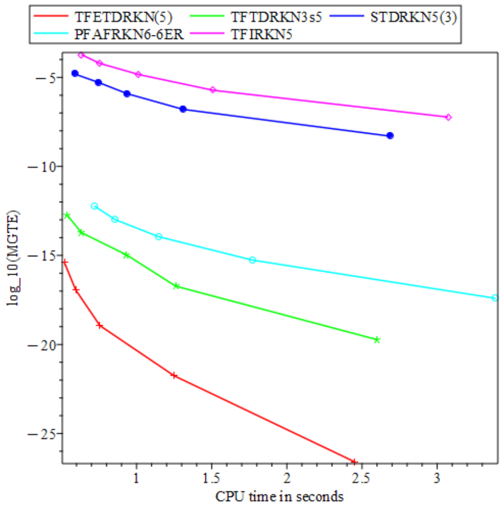

Figure 20: Numerical graph for the experiment 1 with $B = 100$ and $h = 0.025 - 0.005i(i = 0, 1, 2, 3, 4)$.

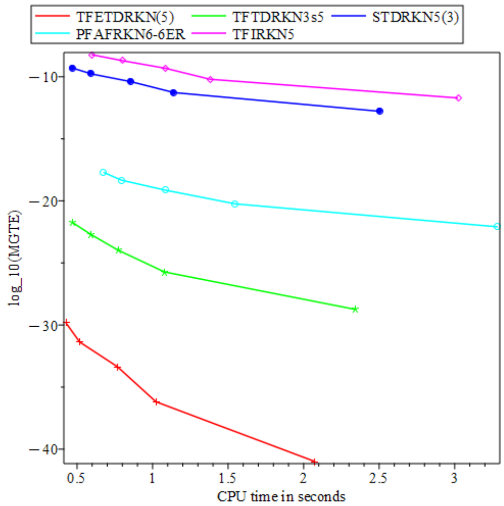

Figure 21: Numerical graph for the experiment 2 with $B = 100$ and $h = 0.025 - 0.005i(i = 0, 1, 2, 3, 4)$.

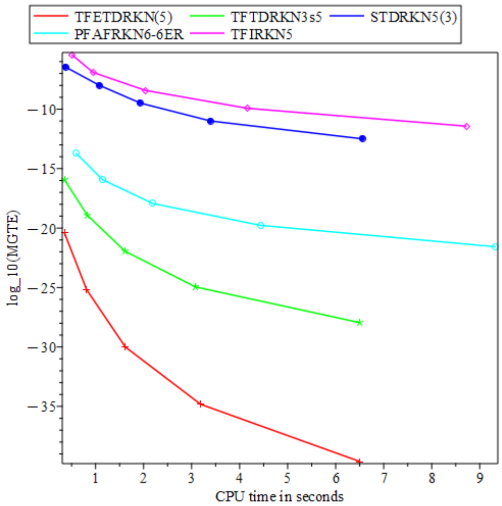

Figure 22: Numerical graph for the experiment 3 with $B = 100$ and $h = 0.1/2^i (i = 0, 1, 2, 3, 4)$.

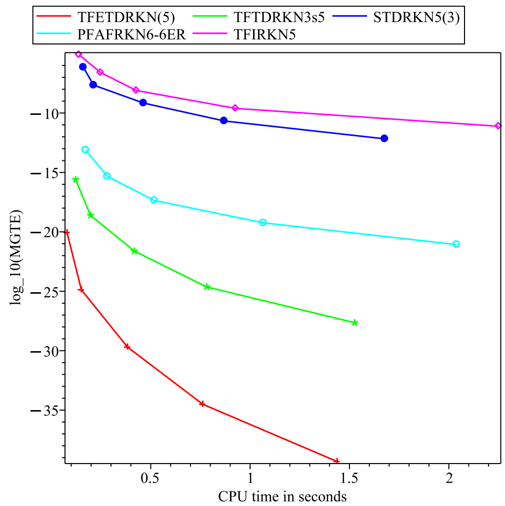

Figure 23: Numerical graph for the experiment 4 with $B = 100$ and $h = 0.1/2^i (i = 0, 1, 2, 3, 4)$.

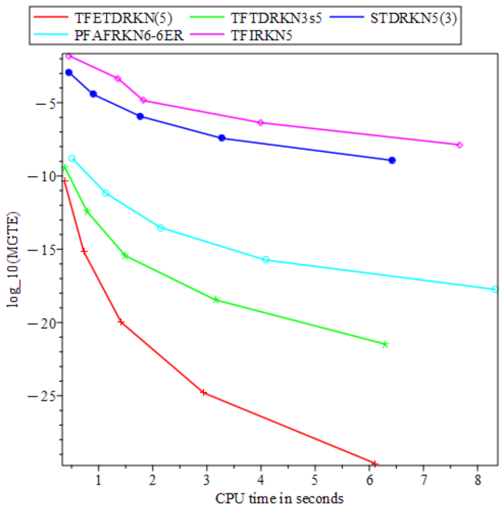

Figure 24: Numerical graph for the experiment 5 with $B = 100$ and $h = 0.1/2^i (i = 0, 1, 2, 3, 4)$.

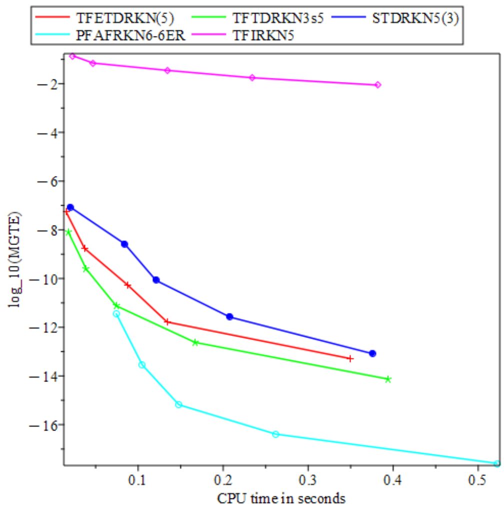

Figure 25: Numerical graph for the experiment 6 with $B = 5$ and $h = 0.1/2^i (i = 0, 1, 2, 3, 4)$.

For the experiments 1 to 5, it is worth noting that the order of increasing values of the MGTE is the TFETDRKN(5), TFTDRKN3s5, PFAFRKN6-6ER, STDRKN, and TFIRKN5 method. An analysis of this phenomenon is provided below. The trigonometrically-fitting technique of the TFETDRKN(5) method is superior to that of the TFTDRKN3s5 for solving first seven special second-order ODEs with periodic solutions like (1), so TFEDTRKN(5) method outperforms TFTDRKN3s5 method. Subsequently, the STDRKN5(3) method is just an efficient TDRKN method without the implementation of trigonometrically-fitting technique, so it certainly performs worst among three TDRKN methods. The reason the PFAFRKN6-6ER method (despite being a sixth-order algebraic method, which would typically result in smaller errors than fifth-order methods) and the TFIRKN5 method (where improvements are generally expected to reduce errors) perform worse than the three above mentioned TDRKN methods is that the TDRKN methods incorporate the second derivative directly into the numerical scheme (3). This integration allows for higher-order accuracy without requiring additional function evaluations, leading to more accurate solutions for the same computational effort compared to the standard RKN methods (see [15]).

Unfortunately, for the experiment 6, from Fig. 25, the TFETDRKN(5) method does not show the best error accuracy but ranks in the middle among the five methods, lagging behind the PFAFRKN6-6ER and the TFTDRKN3s5 method, and better than the STDRKN and the TFIRKN5 method. The PFAFRKN6-6ER method, which performs poorly in error accuracy in the first seven experiments, performs the best in experiment 6, while the TFTDRKN3s5 method performs slightly better than the TFETDRKN(5) method.

The problem in experiment 6 has more secular terms, $u_1(t)\,u_2(t)\,, {u_1}^2(t)$ and ${u_2}^3(t)$, than the other five experiments. The PFAFRKN6-6ER method implements the phase- and amplification-fitted technique during the construction of their method (see further in [13]), which is specifically designed to handle nonlinearities in oscillatory systems. It more accurately captures the phase and amplitude changes caused by the nonlinear term. In the equations shown in the experiment 6, it is the nonlinear terms that causes the amplitude and frequency changes (which is why the frequency λ in Eq 49 depends on ϵ). While, the TFETDRKN(5) method accurately captures periodic behavior through trigonometric fitting and uses second-order derivatives to improve accuracy. However, it is not specifically optimized for nonlinear terms.

The TFETDRKN(5) method is not highly effective for solving second-order systems of ODEs with many nonlinear terms. Consequently, in the simulation of Experiment 6, error accumulation is relatively large compared with the PFAFRKN6 method, and the expected accuracy is not fully achieved. Nevertheless, although the proposed method does not yield the best performance in this case, it still demonstrates significance and value, owing to its lower NTE and reduced computational time (see Table 10) for simulating special second-order systems of ODEs without theoretically periodic solutions.

From all numerical tables, we obtain that when B and h are fixed, the number of function evaluations of the three TDRKN methods are the same, but smaller than that of the PFAFRKN6-6ER (also smaller than the TFIRKN5 method) and the TFIRKN5 method, which is consistent with the relatively low computational complexity of the three TDRKN methods. Also, the computational time of the three TDRKN methods is generally shorter than that of the PFAFRKN6-6ER and TFIRKN5 methods in all experiments, which the reason of is the three TDRKN methods are all two-derivative Runge-Kutta-Nyström methods, where the complexity of a single function evaluation is lower than that of the PFAFRKN6-6ER method which is of sixth order and the TFIRKN5 method which requires the most function evaluations during process.

Overall, the TFETDRKN(5) method outperforms other compared methods when solving special second order (system) ODEs which have theoretical solutions. This is due to its lowest MGTE, which translates to the best accuracy, as well as its relatively better convergence, as well as low number function evaluations and computational time. Hence, the TFETDRKN(5) method outperforms other compared methods about the effectiveness and computational time.

9. Further Study for Real-World Experiment 6

9.1. Theoretical verification of energy preservation for TFETDRKN(5)

Background and notation Consider the second-order Hamiltonian system

$$q''(t) = f(q(t)) = -\nabla U(q(t)), \qquad p := q'.$$

The Hamiltonian (total energy) is

$$H(q,p) = \frac{1}{2}p^T p + U(q).$$

We denote by q_n, p_n the numerical approximations at time t_n and by q_{n+1}, p_{n+1} their one-step updates by the TFETDRKN(5) method with stepsize h. The goal is to prove

$$\Delta H := H(q_{n+1}, p_{n+1}) - H(q_n, p_n) = \mathcal{O}(h^6),$$

i.e. the local energy error is of order h^6 (so energy is preserved up to the method order).

The three-stage two-derivative Runge–Kutta–Nyström update has the form (matching the equation in Hamiltonian system)

$$\begin{aligned} q_{n+1} &= q_n + hp_n + \frac{h^2}{2}f_n + h^3 \sum_{i=1}^{3} \bar{d}_i\, \ell_i, \\ p_{n+1} &= p_n + hf_n + h^2 \sum_{i=1}^{3} \tilde{d}_i\, \ell_i, \end{aligned} \tag{50}$$

where $f_n := f(q_n) = -\nabla U(q_n)$ and each stage evaluation ℓ_i is a shorthand for the two-derivative evaluation at the i-th stage,

$$\ell_i = g\big(t_n + c_i h,\ U_i,\ U_i'\big),$$

and the stages U_i, U_i' depend on $q_n, p_n, f_n, \{\bar{A}_{ij} and \tilde{A}_{ij}\}$. For the algebra below it suffices that the method coefficients $\{c_i, \bar{A}_{ij}, \tilde{A}_{ij}, \bar{d}_i, \tilde{d}_i\}$ satisfy the ETDRKN(5) order conditions (these will be used to cancel coefficient combinations).

Step 1: Expand the kinetic energy term. Compute the kinetic part at $n+1$:

$$\begin{aligned}\frac{1}{2}p_{n+1}^T p_{n+1} &= \frac{1}{2}\Big(p_n + hf_n + h^2\sum_i \tilde{d}_i\ell_i\Big)^T\Big(p_n + hf_n + h^2\sum_j \tilde{d}_j\ell_j\Big)\\ &= \frac{1}{2}p_n^T p_n + h\,p_n^T f_n + \frac{h^2}{2}f_n^T f_n\\ &\quad + h^2 p_n^T\sum_i \tilde{d}_i\ell_i + h^3 f_n^T\sum_i \tilde{d}_i\ell_i + \frac{h^4}{2}\Big(\sum_i \tilde{d}_i\ell_i\Big)^T\Big(\sum_j \tilde{d}_j\ell_j\Big).\end{aligned}$$

Retain all terms up to order h^5 (the last displayed term is $O(h^4\cdot\ell^2)$; since we assume $\ell = O(1)$ these terms are of order $O(h^4)$ or higher).

Step 2: Expand the potential energy term. Taylor-expand $U(q_{n+1})$ about q_n. Using (50) write

$$\Delta q := q_{n+1} - q_n = hp_n + \frac{h^2}{2}f_n + h^3\sum_i \bar{d}_i\ell_i,$$

and expand:

$$U(q_{n+1}) = U(q_n) + \nabla U(q_n)^T\Delta q + \frac{1}{2}\Delta q^T\nabla^2 U(q_n)\,\Delta q + \frac{1}{6}D^3U(q_n)[\Delta q,\Delta q,\Delta q] + \mathcal{O}(\|\Delta q\|^4).$$

Substitute Δq; using $f_n = -\nabla U(q_n)$ we get

$$\begin{aligned}U(q_{n+1}) &= U(q_n) + h\nabla U(q_n)^T p_n + \frac{h^2}{2}\nabla U(q_n)^T f_n + h^3\nabla U(q_n)^T\sum_i \bar{d}_i\ell_i\\ &\quad + \frac{h^2}{2}p_n^T\nabla^2 U(q_n)p_n + h^3 p_n^T\nabla^2 U(q_n)\,\frac{h}{2}f_n + \mathcal{O}(h^3\cdot h^3).\end{aligned}$$

Retain terms up to order h^5; higher-order terms will be grouped later into $\mathcal{O}(h^6)$.

Step 3: Assemble ΔH and identify grouped terms. Using the expansions above,

$$\begin{aligned}\Delta H &= \Big(\frac{1}{2}p_{n+1}^T p_{n+1} - \frac{1}{2}p_n^T p_n\Big) + \big(U(q_{n+1}) - U(q_n)\big)\\ &= \Big[hp_n^T f_n + \frac{h^2}{2}f_n^T f_n + h^2 p_n^T\sum_i \tilde{d}_i\ell_i + h^3 f_n^T\sum_i \tilde{d}_i\ell_i + \frac{h^4}{2}\|\sum_i \tilde{d}_i\ell_i\|^2\Big]\\ &\quad + \Big[h\nabla U(q_n)^T p_n + \frac{h^2}{2}\nabla U(q_n)^T f_n + h^3\nabla U(q_n)^T\sum_i \bar{d}_i\ell_i\\ &\qquad + \frac{h^2}{2}p_n^T\nabla^2 U(q_n)p_n + h^3(\text{other } p_n, f_n \text{ mixed terms})\Big] - h\,p_n^T\nabla U(q_n) + \mathcal{O}(h^6).\end{aligned}$$

Now use $f_n = -\nabla U(q_n)$. Several cancellations are immediate:
- The $O(h)$ terms cancel:

$$hp_n^T f_n + h\nabla U(q_n)^T p_n - hp_n^T \nabla U(q_n) = 0.$$

- Combine $O(h^2)$ terms. Replace $\nabla U(q_n)$ by $-f_n$ where convenient:

$$\begin{aligned}&\frac{h^2}{2} f_n^T f_n + \frac{h^2}{2}\nabla U(q_n)^T f_n + h^2 p_n^T \sum_i \tilde{d}_i \ell_i + \frac{h^2}{2} p_n^T \nabla^2 U(q_n) p_n \\ &= \frac{h^2}{2} f_n^T f_n - \frac{h^2}{2} f_n^T f_n + h^2 p_n^T \sum_i \tilde{d}_i \ell_i + \frac{h^2}{2} p_n^T \nabla^2 U(q_n) p_n \\ &= h^2 p_n^T \sum_i \tilde{d}_i \ell_i + \frac{h^2}{2} p_n^T \nabla^2 U(q_n) p_n.\end{aligned}$$

The two first terms cancel exactly. The remaining h^2 expression involves p_n and stage contributions ℓ_i. These are not yet zero but will be converted (via integration-by-parts like manipulations using the stage definitions) into a symmetric bilinear form in the stage forces $f(Q.)$ with kernel given below.

After collecting all terms up to order h^5 and doing the routine algebra (expand stages U_i, U_i' in Taylor series about (q_n, p_n), replace stage ℓ_i by their expansions in terms of f_n and derivatives), the change in energy can be written in the compact bilinear form

$$\Delta H \;=\; \frac{h^2}{2} \sum_{r,s=0}^{5} h^r h^s \, \mathcal{C}_{rs}(q_n, p_n) \;=\; \frac{h^2}{2} \iint_{[0,1]^2} f(Q_\tau)^T \, D(\tau, \sigma; v) \, f(Q_\sigma) \, d\sigma d\tau \;+\; \mathcal{O}(h^6), \tag{51}$$

where $D(\tau, \sigma; v)$ is the kernel

$$D(\tau, \sigma; v) \;:=\; B_\tau(v) B_\sigma(v) - \partial_\tau A_{\tau\sigma}(v) - \partial_\sigma A_{\sigma\tau}(v),$$

and $A_{\tau\sigma}, B_\tau$ are the continuous kernels associated with the method coefficients (discrete collocation/quadrature reproduces these at nodes c_i). The representation (51) is standard in continuous-stage proofs: the h^2-term collects into a symmetric double integral in the stage forces $f(Q.)$ with kernel D; higher-order contributions (from cubic and quartic expansions) are absorbed into $\mathcal{O}(h^6)$ once the method order conditions are used.

Step 4: Interpretation of the kernel D and sufficient condition for energy preservation. Equation (51) shows that the leading nontrivial contribution to ΔH is the h^2-term with kernel D. Therefore a *sufficient* and (for arbitrary f) necessary condition to annihilate that leading term is

$$B_\tau(v) B_\sigma(v) \;=\; \partial_\tau A_{\tau\sigma}(v) + \partial_\sigma A_{\sigma\tau}(v) \qquad \text{for all } \tau, \sigma \in [0, 1]. \tag{52}$$

If (52) holds pointwise, the h^2-term vanishes. (This is the continuous-stage identity analogous to the discrete condition you quoted; for discrete nodes it becomes $B_i B_j = \partial_\tau A_{\tau\sigma}|_{(\tau,\sigma)=(c_i,c_j)} + \cdots$.)

Step 5: Cancellation of Higher-Order Terms via Order Conditions After the h^2-term is removed by (52), the remaining contributions in ΔH are of higher powers of h. A careful expansion shows that the next orders that may survive are h^3, h^4, h^5; each of these is a finite linear combination of the method coefficients multiplying derivatives/compositions of f and U evaluated at the stages. Crucially, those linear combinations are exactly the order conditions for the ETDRKN(5) method (the conditions you solved to obtain the coefficients: the third–sixth order conditions for q and second–sixth for p, plus the simplifying assumptions). Because TFETDRKN(5) was constructed so that these order conditions hold, each of the algebraic coefficient combinations multiplying the h^3, h^4, h^5 contributions is zero.

Therefore, when the method coefficients satisfy:

- the trigonometrically-fitted stage/exponential relations (which algebraically imply (52)), and
- the ETDRKN(5) order conditions (which annihilate the h^3, h^4, h^5 coefficient combinations),

then all contributions to ΔH up to order h^5 vanish identically. The first possibly nonzero term is of order h^6. Symbolically,

$$\Delta H = \mathcal{O}(h^6).$$

Step 6: Discrete-stage remark (collocation/nodes). In practice we work with the discrete three-stage TFETDRKN(5) tableau: the continuous kernels $A_{\tau\sigma}, B_\tau$ are sampled at the nodes $\tau, \sigma \in \{c_1, c_2, c_3\}$ and replaced by the discrete coefficients $\bar{A}_{ij}(w), \tilde{A}_{ij}(w), \bar{d}_i(w), \tilde{d}_i(w)$ (frequency dependent). The same chain of algebra applies: substitute the discrete formulas (for example $\bar{A}_{21}(w) = (c_2 w - \sin(c_2 w))/w^3$, $\tilde{A}_{21}(w) = (1 - \cos(c_2 w))/w^2$, etc.) into the discrete analog of the kernel $D_{ij}(w)$:

$$D_{ij}(w) := B_i(w)B_j(w) - \big(\partial_\tau A_{\tau\sigma}(w) + \partial_\sigma A_{\sigma\tau}(w)\big)\Big|_{(\tau,\sigma)=(c_i,c_j)}.$$

Expanding $D_{ij}(w)$ in a Taylor series in w shows $D_{ij}(w) = \mathcal{O}(w^8)$ (i.e. zero up to w^6) because the trigonometrical fitting identities were enforced exactly and the order conditions annihilate the lower-order terms. Hence the discrete local energy error is $\mathcal{O}(h^6)$ as well.

Conclusion. Combining the continuous algebra with the discrete collocation sampling used to obtain TFETDRKN(5) coefficients, we conclude that the TFETDRKN(5) method satisfies

$$\Delta H = H(q_{n+1}, p_{n+1}) - H(q_n, p_n) = \mathcal{O}(h^6).$$

provided the method coefficients are chosen to satisfy the trigonometrical reproduction identities and the ETDRKN(5) order conditions. This proves that TFETDRKN(5) preserves the Hamiltonian up to (and including) order five; the leading energy error term is of order h^6.

□

Definition 5 ([32])**.** *A Hamiltonian system with n-degree of freedom is characterized by*

$$\frac{dv_1}{dt} = \frac{\partial H}{\partial u_1}, \ \frac{dv_2}{dt} = \frac{\partial H}{\partial u_2}, \cdots, \ \frac{dv_n}{dt} = \frac{\partial H}{\partial u_n}; \ \frac{du_1}{dt} = \frac{\partial H}{\partial v_1}, \ \frac{du_2}{dt} = \frac{\partial H}{\partial v_2}, \cdots, \frac{du_n}{dt} = \frac{\partial H}{\partial v_n}, \tag{53}$$

where H is the Hamiltonian energy of the system. In real-word applications, $u_i\,(i = 1, \cdots, n)$ represent the generalized coordinates and $v_i\,(i = 1, \cdots, n)$ are generalized momentum.

Definition 6. *The Hamiltonian and Lagrangian energy can be expressed as, respectively*

$$\begin{aligned} H(u, v; t) &= T_E(v; t) + V_E(u; t), \\ L(u, v; t) &= T_E(v; t) - V_E(u; t), \end{aligned} \tag{54}$$

where T_E and V_E are the kinetic and potential energies, respectively. So it is convenient to characterized a Hamiltonian system with 2-degree of freedom, the Hamiltonian and Lagrangian energy, respectively

$$\begin{aligned} H(u_1, u_2, v_1, v_2; t) &= T_E(v_1, v_2; t) + V_E(u_1, u_2; t), \\ L(u_1, u_2, v_1, v_2; t) &= T_E(v_1, v_2; t) - V_E(u_1, u_2; t). \end{aligned} \tag{55}$$

Definition 7. *If the kinetic energy $T_E(v_1, v_2; t)$ of a Hamiltonian system with 2-degree of freedom (55) has a standard quadratic form such as:*

$$T_E(v_1, v_2; t) = \frac{1}{2m_1}{v_1}^2 + \frac{1}{2m_2}{v_2}^2, \tag{56}$$

where v_1 and v_2 are the generalized momentum mentioned above (55), m_1 and m_2 are the masses associated with each degree of freedom, respectively. Then the concrete expression of momentum of the Hamiltonian system with 2-degree of freedom (55) can be expressed as

$$p_1 = m_1\frac{du_1}{dt}, \ p_2 = m_2\frac{du_2}{dt}, \tag{57}$$

where $\frac{du_1}{dt}$ and $\frac{du_2}{dt}$ are the corresponding velocities, then p_1 and p_2 represent the linear momentum corresponding to these velocities.

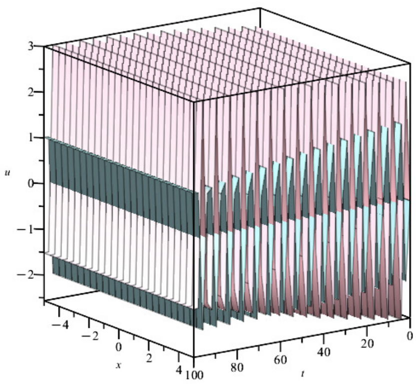

Figure 26: 3D theoretical phase for experiment 6 with $h = 0.125$ and $t \in [0, 100]$.

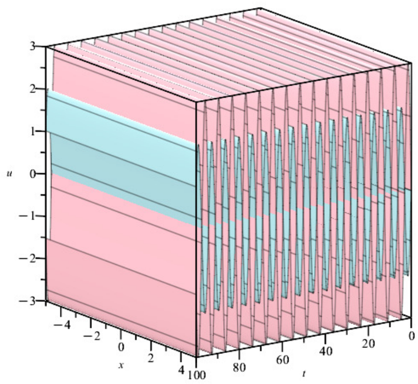

Figure 27: 3D numerical phase for experiment 6 with $h = 0.125$ and $t \in [0, 100]$.

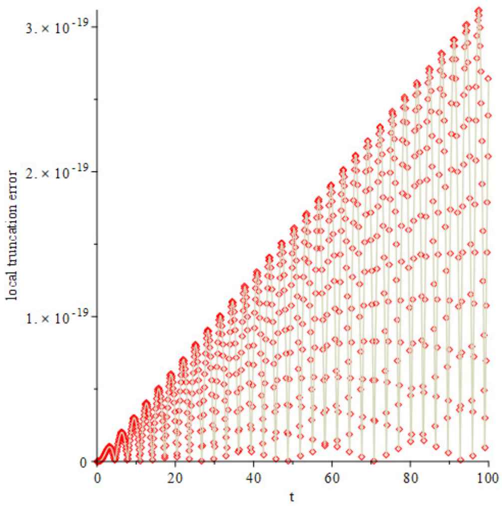

Figure 28: LTE for experiment 6 with $h = 0.125$ and $t \in [0, 100]$.

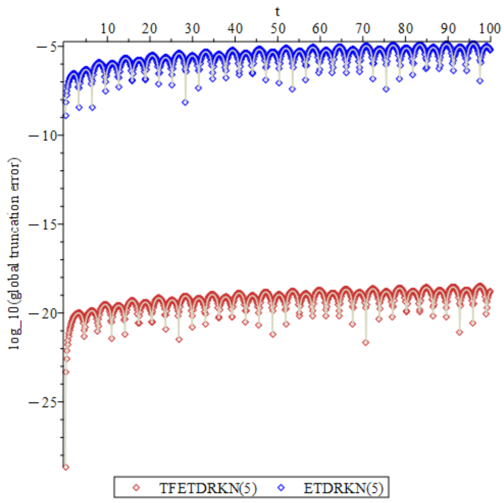

Figure 29: Comparison phase of two methods for experiment 6 with $h = 0.125$ and $t \in [0, 100]$.

In this section, we conduct a detailed investigation of real-world experiment 6 to demonstrate the superiority of the TFETDRKN(5) method in terms of accuracy and energy conservation, achieved through the use of the trigonometrical integration technique. Figs. 26-28 visualize the theoretical and numerical solutions of experiment 6 and the absolute value of their differences. Fig. 28 displays how the LTE changes during the integration process from $t = 0$ to $t = 100$. Note that LTE doesn't decrease linearly but with oscillatory behavior, in the meanwhile, the oscillation amplitude is regular. The reasons for these two phenomena are that the displacement change of two cars in experiment 6 behaves in an oscillatory manner and the two ODEs of experiment 6 is linear. Also, Fig. 29 illustrates the superiority of the accuracy of trigonometrical integration technique through comparing the LTEs generated by the ETDRKN(5) and TFETDRKN(5) methods, respectively.

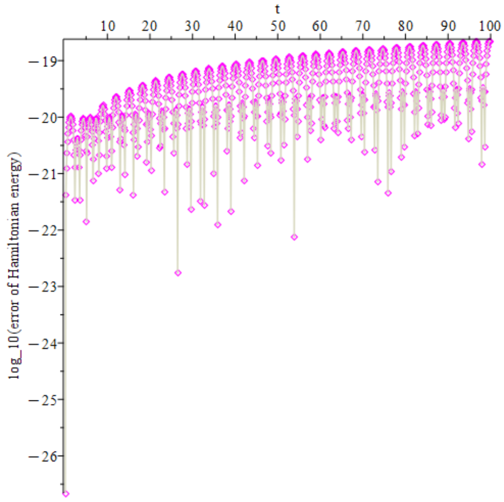

Figure 30: Hamiltonian energy conversation for the experiment 6 with $h = 0.125$ and $t \in [0, 100]$.

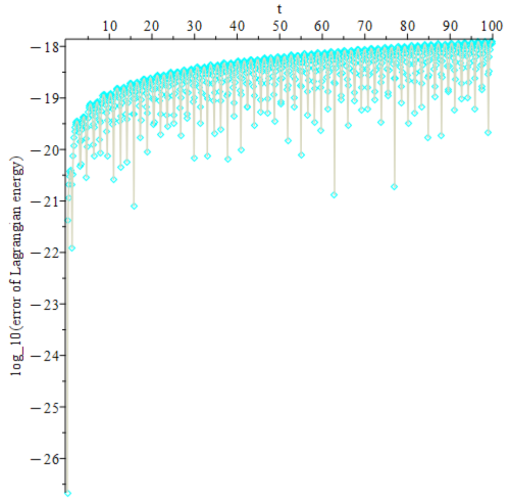

Figure 31: Lagrangian energy conversation for the experiment 6 with $h = 0.125$ and $t \in [0, 100]$.

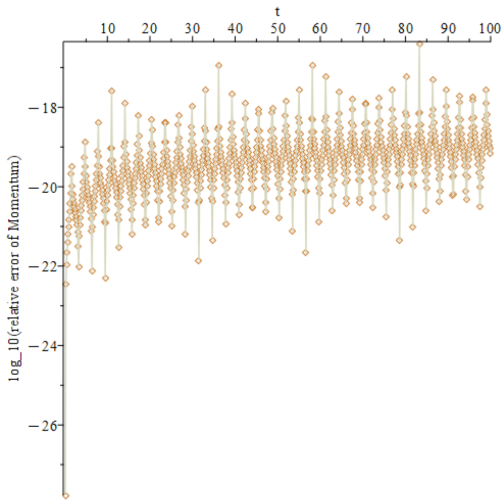

Figure 32: Momentum conversation for experiment the 6 with $h = 0.125$ and $t \in [0, 100]$.

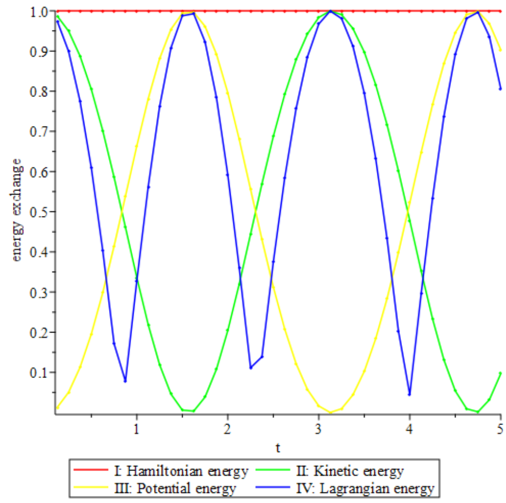

Figure 33: Relative energy exchange for the experiment 6 with $h = 0.125$ and $t \in [0, 5]$.

Subsequently, Figs. 30-32 visually illustrate the superior performance of the Hamiltonian energy, Lagrangian energy, and momentum conservation in experiment 6, using the TFETDRKN(5) method with $h = 0.125$ and $t \in [0, 100]$. It should be noted that these three errors do not exhibit a linear increase but rather display an oscillatory behavior due to the oscillatory manner of the system's ODEs in experiment 6. As time t progresses from 1 to 100, the already small relative errors increase in an oscillatory manner, further highlighting their stability. At last, Fig. 33 shows the relative energy exchange process with $h = 0.125$ and $t \in [0, 5]$ for the experiment 6. Throughout the process, the three quantities exhibit a regular, periodic behavior, most notably following an oscillatory pattern resembling sine and cosine functions like $\sin(t)$ and $\cos(t)$, as they evolve over time.

10. Conclusions

In this paper, we proposed a new three-stage and fifth-order TFETDRKN(5) method, based initially on the construction of the ETDRKN(5) method. We performed an detailed stability analysis of the TFETDRKN(5) method including stability matrix, dispersion and dissipation error analysis and stability properties and regions. We derived the stability matrix and decided to conduct the stability analysis considering two cases, $\lambda = \mu$ and $\lambda \neq \mu$. In this case, the dispersion and the dissipation error were introduced, followed by the presentation of the necessary and sufficient conditions. It was then proven that the TFETDRKN(5) method achieves dispersion of order 2 and dissipation of order 3. For the case, $\lambda = \mu$, we defined and plotted the stability region, then illustrated the stability property for the TFETDRKN(5) method. Stability interval was introduced and calculated, $(-1.588, 0)$. For the other case, $\lambda \neq \mu$, we similarly defined and plotted the periodicity stability region, then analysed the stability property of characteristic polynomial for the TFETDRKN(5) method. After that, we proved that the ETDRKN(5) method is algebraic of order 5. Importantly, to evaluate the numerical effectiveness and accuracy of the TFETDRKN(5) method, we performed numerical tests on the first seven experiments with theoretically periodic solutions, and on experiment 6, which lacks a periodic solution. The new proposed method was compared with four selected existing methods by plotting the MGTE against the step size, h. The results of tables and graphs and discussion demonstrated that the TFETDRKN(5) method outperforms other compared methods by producing nearly the least absolute maximum global truncation error (except for experiment 6) , relatively small time of computations and relatively less (the same as the other TDRKN methods) number of function evaluations in experiments 1 to 5. Despite not achieving the lowest numerical MGTE, the new method proved crucial for simulating special second order (system) ODEs like those in experiment 6, which lack theoretical solutions. We further extended our study of experiment 6, and the results show that the TFETDRKN(5) method significantly outperforms the EDTKRN(5) method, following the application of the trigonometrically-fitting technique. By comparing the global truncation errors over time, the superiority of the TFETDRKN(5) becomes evident. Moreover, the proposed method successfully preserves the energy conservation property.

For future research, some new two-derivative Runge-Kutta-Type methods can be developed specifically for solving third-order ODEs. Even though some third-order ODEs can be decomposed into first-order or second-order ODEs to be solved using the proposed method in this paper (or other articles), this will increase computational complexity and make the process more cumbersome. Meanwhile, no one has studied the two-derivative Runge-Kutta-Nyström methods for solving third-order ODEs. So in the future, we can focus on developing the two-derivative Runge-Kutta-Nyström methods for solving third-order ODEs with periodic solutions, even exponential solutions based on our study.

Acknowledgements

This study is supported by the Grant Scheme (Ref. No. GGPM-2023-029) from Universiti Kebangsaan Malaysia.

Declaration of competing interest

The authors declare no conflict of interest.

References

[1] R. P. Agarwal, S. R. Grace, and D. O'Regan. *Oscillation theory for second order dynamic equations*. CRC Press, 2002.

[2] M. Condon, A. Deaño, and A. Iserles. On highly oscillatory problems arising in electronic engineering. *ESAIM: Mathematical Modelling and Numerical Analysis*, 43(4):785–804, 2009.

[3] R. Ciii. About the numerical solution of differential equations. *Mathematical Annals*, 46(2):167–178, 1895.

[4] K. Wiii. Contribution to the approximate integration of total differential equations. *Mathematical Annals*, 45(1):435–453, 1901.

[5] E. J. Nyström. About the numerical integration of differential equations. *Fennic Society of Sciences*, 50(13):1–55, 1925.

[6] B. Paternoster. Runge-Kutta-Nyström methods for ODEs with periodic solutions based on trigonometric polynomials. *Applied Numerical Mathematics*, 28(2-4):401–412, 1998.

[7] P. Albrecht. The extension of the theory of a-methods to rk methods. In *Numerical Treatment of Differential Equations, Proceedings 4th Seminar NUMDIFF*, volume 4, pages 9–18, 1987.

[8] J. M. Franco. Runge-Kutta-Nyström methods adapted to the numerical integration of perturbed oscillators. *Computer Physics Communications*, 147(3):770–787, 2002.

[9] J. Li. Trigonometrically fitted three-derivative runge–kutta methods for solving oscillatory initial value problems. *Applied Mathematics and Computation*, 330:103–117, 2018.

[10] J. Li, S. Deng, and X. Wang. Extended explicit pseudo two-step rkn methods for oscillatory systems $y'' + my = f(y)$. *Numerical Algorithms*, 78:673–700, 2018.

[11] M. A. Demba, N. Senu, and F. Ismail. Trigonometrically-fitted explicit four-stage fourth-order Runge-Kutta-Nyström method for the solution of initial value problems with oscillatory behavior. *Global Journal of Pure and Applied Mathematics*, 12(1):67–80, 2016.

[12] M. A. Demba, N. Senu, and F. Ismail. An embedded 4 (3) pair of explicit trigonometrically-fitted Runge-Kutta-Nyström method for solving periodic initial value problems. *Appl. Math. Sci*, 11:819–838, 2017.

[13] M. A. Demba, H. Ramos, P. Kumam, and W. Watthayu. A phase-fitted and amplification-fitted explicit Runge-Kutta-Nyström pair for oscillating systems. *Mathematical and Computational Applications*, 26(3):59, 2021.

[14] M. A. Demba, N. Senu, H. Ramos, P. Kumam, and W. Watthayu. A phase-and amplification-fitted 5 (4) diagonally implicit Runge-Kutta-Nyström pair for oscillatory systems. *Bulletin of the Iranian Mathematical Society*, 49(3):24, 2023.

[15] Z. Chen, Z. Qiu, J. Li, and X. You. Two-derivative Runge-Kutta-Nyström methods for second-order ordinary differential equations. *Numerical Algorithms*, 70:897–927, 2015.

[16] S. N. Jator. Implicit third derivative Runge-Kutta-Nyström method with trigonometric coefficients. *Numerical Algorithms*, 70:133–150, 2015.

[17] Z. Chen, L. Shi, S. Liu, and X. You. Trigonometrically fitted two-derivative runge-kutta-nyström methods for second-order oscillatory differential equations. *Applied Numerical Mathematics*, 142:171–189, 2019.

[18] T. S. Mohamed, N. Senu, Z. B. Ibrahim, and N. M. A. Nik Long. Efficient two-derivative Runge-Kutta-Nyström methods for solving general second-order ordinary differential equations. *Discrete Dynamics in Nature and Society*, 2018, 2018.

[19] J. O. Ehigie, M. Zou, X. Hou, and X. You. On modified TDRKN methods for second-order systems of differential equations. *International Journal of Computer Mathematics*, 95(1):159–173, 2018.

[20] K. C. Lee, M. A. Alias, N. Senu, and A. Ahmadian. On efficient frequency-dependent parameters of explicit two-derivative improved Runge-Kutta-Nyström method with application to two-body problem. *Alexandria Engineering Journal*, 72:605–620, 2023.

[21] G. Xue and Y. Ye. An efficient algorithm for minimizing a sum of euclidean norms with applications. *SIAM Journal on Optimization*, 7(4):1017–1036, 1997.

[22] H. Ramos and J. Vigo-Aguiar. On the frequency choice in trigonometrically fitted methods. *Applied Mathematics Letters*, 23(11):1378–1381, 2010.

[23] P. J. Van der Houwen and B. P. Sommeijer. Diagonally implicit Runge-Kutta-nyström methods for oscillatory problems. *SIAM Journal on Numerical Analysis*, 26(2):414–429, 1989.

[24] M. A. Demba, H. Ramos, P. Kumam, and W Watthayu. An optimized sixth-order explicit RKN method to solve oscillating systems. In *Proceedings of the XXVI Congreso de Ecuaciones Diferenciales y Aplicaciones. XVI Congreso de Matemática Aplicada*. Servicio de Publicaciones de la Universidad de Oviedo, 2021.

[25] W. J. Hasan and K. A. Hussain. Fifth order improved Runge-Kutta-Nystrom method using trigonometrically-fitting for solving oscillatory problems. *Al-Nahrain Journal*

of Science, 25(4):63–67, 2022.

[26] B. S. Attili, K. Furati, and M. I. Syam. An efficient implicit Runge-Kutta method for second order systems. *Applied Mathematics and Computation*, 178(2):229–238, 2006.

[27] D. O. Awoyemi. A p-stable linear multistep method for solving general third order ordinary differential equations. *International Journal of Computer Mathematics*, 80(8):985–991, 2003.

[28] J. M. Franco, I. Gómez, and L. Rández. Four-stage symplectic and p-stable SDIRKN methods with dispersion of high order. *Numerical Algorithms*, 26:347–363, 2001.

[29] J. Lebl. *Notes on diffy Qs: differential equations for engineers.* Independent, 2014.

[30] X. Wu and B. Wang. *Geometric integrators for differential equations with highly oscillatory solutions.* Springer, 2021.

[31] J. Vigo-Aguiar, T. E. Simos, and J. M. Ferrándiz. Controlling the error growth in long–term numerical integration of perturbed oscillations in one or several frequencies. *Proceedings of the Royal Society of London. Series A: Mathematical, Physical and Engineering Sciences*, 460(2042):561–567, 2004.

[32] S. Lynch. *Dynamical systems with applications using MAPLE.* Springer, 2010.

Appendices

Frequency-Dependent Coefficients of Two-Derivative Runge-Kutta-Nyström Method

$$
\begin{aligned}
\bar{A}_{21}(w) &= \frac{1}{30}+\frac{\sqrt{5}}{75}+\left(-\frac{1}{1200}-\frac{11\sqrt{5}}{30000}\right)w^2+\left(\frac{13}{1260000}+\frac{29\sqrt{5}}{6300000}\right)w^4+\left(-\frac{17}{226800000}-\frac{19\sqrt{5}}{567000000}\right)w^6\\
&\quad+\left(\frac{89}{249480000000}+\frac{199\sqrt{5}}{1247400000000}\right)w^8+O\left(w^{10}\right),\\
\bar{A}_{32}(w) &= \frac{98209}{2714430}-\frac{\sqrt{5}}{75}+\left(\frac{136849}{108577200}+\frac{476881\sqrt{5}}{2714430000}\right)w^2+\left(\frac{11338513}{57003030000}+\frac{4109663\sqrt{5}}{57003030000}\right)w^4+\\
&\quad\left(\frac{79811269}{2052109080000}+\frac{1733239283\sqrt{5}}{102605454000000}\right)w^6+\left(\frac{184081799677}{22573199880000000}+\frac{409862403109\sqrt{5}}{112865999400000000}\right)w^8+O\left(w^{10}\right),\\
\bar{\chi}_2(w) &= 1+\frac{1}{240000}\left(5+\sqrt{5}\right)^4w^4-\frac{1}{720000000}\left(5+\sqrt{5}\right)^6w^6+\frac{1}{4032000000000}(5+\sqrt{5})^8w^8+O\left(w^{10}\right),\\
\bar{\chi}_3(w) &= 1+\left(-\frac{121393}{21715440}+\frac{59569\sqrt{5}}{108577200}\right)w^4+\left(-\frac{1019767}{2035822500}-\frac{214129\sqrt{5}}{1628658000}\right)w^6+\\
&\quad\left(-\frac{394695169}{4560242400000}-\frac{163481333\sqrt{5}}{4560242400000}\right)w^8+O\left(w^{10}\right),\\
\tilde{A}_{21}(w) &= \frac{3}{20}+\frac{\sqrt{5}}{20}+\left(-\frac{7}{1200}-\frac{\sqrt{5}}{400}\right)w^2+\left(\frac{1}{10000}+\frac{\sqrt{5}}{22500}\right)w^4+\left(-\frac{47}{50400000}-\frac{\sqrt{5}}{2400000}\right)w^6+\\
&\quad\left(\frac{41}{7560000000}+\frac{11\sqrt{5}}{4536000000}\right)w^8+O\left(w^{10}\right),\\
\tilde{A}_{32}(w) &= \frac{3}{20}-\frac{\sqrt{5}}{20}+\left(\frac{1}{240}+\frac{\sqrt{5}}{400}\right)w^2+\left(\frac{11}{10000}+\frac{41\sqrt{5}}{90000}\right)w^4+\left(\frac{2281}{10080000}+\frac{241\sqrt{5}}{2400000}\right)w^6+\\
&\quad\left(\frac{361961}{7560000000}+\frac{97009\sqrt{5}}{4536000000}\right)w^8+O\left(w^{10}\right),\\
\tilde{\chi}_2(w) &= 1-\frac{1}{600}\left(5+\sqrt{5}\right)^2w^2+\frac{1}{1200000}\left(5+\sqrt{5}\right)^4w^4-\frac{1}{5040000000}\left(5+\sqrt{5}\right)^6w^6+\\
&\quad\frac{1}{36288000000000}(5+\sqrt{5})^8w^8+O\left(w^{10}\right),\\
\tilde{\chi}_3(w) &= 1+\left(\frac{1}{20}+\frac{\sqrt{5}}{60}\right)^2w^2+\left(\frac{-29\sqrt{5}-75}{-15000+3000\sqrt{5}}\right)w^4+\left(\frac{-683\sqrt{5}-1560}{-1575000+315000\sqrt{5}}\right)w^6+\\
&\quad\frac{1}{226800000}\frac{-105209\sqrt{5}-235985}{-5+\sqrt{5}}w^8+O\left(w^{10}\right).
\end{aligned}
\tag{58}
$$

$$
\begin{aligned}
\bar{d}_2(w) &= -\frac{\sqrt{5}}{48} + \frac{1}{16} + \left(\frac{\sqrt{5}}{504000} - \frac{1}{201600}\right) w^4 + \left(-\frac{\sqrt{5}}{181440000} - \frac{1}{181440000}\right) w^6 + \\
&\quad \left(\frac{\sqrt{5}}{66528000000} - \frac{17}{39916800000}\right) w^8 + O\left(w^{10}\right), \\
\bar{d}_3(w) &= \frac{\sqrt{5}}{48} + \frac{1}{16} + \left(-\frac{\sqrt{5}}{504000} - \frac{1}{201600}\right) w^4 + \left(\frac{\sqrt{5}}{181440000} - \frac{1}{181440000}\right) w^6 + \\
&\quad \left(-\frac{\sqrt{5}}{66528000000} - \frac{17}{39916800000}\right) w^8 + O\left(w^{10}\right), \\
\tilde{d}_2(w) &= -\frac{\sqrt{5}}{24} + \frac{5}{24} + \frac{1}{252000}\sqrt{5} w^4 + \left(-\frac{\sqrt{5}}{90720000} + \frac{1}{6048000}\right) w^6 + \left(\frac{\sqrt{5}}{33264000000} + \frac{1}{362880000}\right) w^8 + O\left(w^{10}\right), \\
\tilde{d}_3(w) &= \frac{\sqrt{5}}{24} + \frac{5}{24} - \frac{1}{252000}\sqrt{5} w^4 + \left(\frac{\sqrt{5}}{90720000} + \frac{1}{6048000}\right) w^6 + \left(-\frac{\sqrt{5}}{33264000000} + \frac{1}{362880000}\right) w^8 + O\left(w^{10}\right).
\end{aligned}
\tag{59}
$$